AD 287 889

USAERADL Technical Report 2292

NUCLEAR PULSE EFFECTS IN CABLES

Kurt Ikrath

Randolph Constantine

August 1962

UNITED STATES ARMY
ELECTRONICS RESEARCH AND DEVELOPMENT LABORATORY
FORT MONMOUTH, N.J.

U.S. ARMY ELECTRONICS RESEARCH AND DEVELOPMENT LABORATORY
FORT MONMOUTH, NEW JERSEY

August 1962

USAERADL Technical Report 2292 has been prepared under the supervision of the Institute for Exploratory Research, and is published for the information and guidance of all concerned. Suggestions or criticisms relative to the form, contents, purpose, or use of this publication should be referred to the U.S. Army Electronics Research and Development Laboratory, Fort Monmouth, New Jersey, Attn: Director, Exploratory Research Division "C".

J. M. KIMBROUGH, JR.
Colonel, Signal Corps
Commanding

OFFICIAL:
H. W. KILLAM
Major, SigC
Adjutant

DISTRIBUTION:
Special

Qualified requesters may obtain copies of this report from ASTIA.

This report has been released to the Office of Technical Services, U. S. Department of Commerce, Washington 25, D. C., for sale to the general public.

NUCLEAR PULSE EFFECTS IN CABLES

Kurt Ikrath and Randolph Constantine

DA TASK NR. 3A99-25-003-02

ABSTRACT

An equivalent circuit for a piece of cable is developed and the differential equations of this circuit are solved under the conditions of a transient burst of nuclear radiation and under various ranges of cable bias voltage. Graphs of representative cases are presented and compared to experimental results. A method of solving for the transient change in cable parameters is given and sample calculations are shown.

U.S. ARMY ELECTRONICS RESEARCH AND DEVELOPMENT LABORATORY

FORT MONMOUTH, NEW JERSEY

CONTENTS

FIGURES

Contents, cont'd.

NUCLEAR PULSE EFFECTS IN CABLES

INTRODUCTION

The effects of nuclear radiation upon electronic systems and components have been a subject of growing interest. The early investigators found two basic types of phenomena, each posing a separate problem; the permanent and the transient damage. Studies of the transient effects of a burst, or pulse of radiation, upon an electronic component have revealed many effects[1] not yet fully understood.

Transmission lines, especially coaxial cables, have a unique role in the investigation of such transient radiation effects. These lines form the link of the components being irradiated to the remote measuring and recording apparatus. Hence, these cables are partially irradiated, and the observed effects upon the components become a composite of component and cable effects. These effects must be isolated from each other either by compensating circuitry in the test network, or by analysis. The investigator must have an exact knowledge of the behavior of cable parameters, i.e., specific conductance, capacitance, inductance, and resistance as a function of the type of nuclear radiation, the time-intensity shape, and the distance intensity distribution of the radiation.

Experimental observations, compared with the data deduced from a theoretical model which is capable of giving an accurate description of the radiation phenomena in terms of electrical circuit parameters, will yield the knowledge required to separate the component effects from the cable effects. Conclusions may be drawn from the behavior of these parameters concerning the material changes affected by the nuclear irradiation. Such a theoretical model for transient nuclear radiation effects in cables is given here. This model is capable of resolving the observed voltage or current transient into the corresponding electrical cable parameters.

DISCUSSION

A. The Lumped-Circuit Approach

The theoretical model is derived from network theory. When this theory is applied to transients in electrical networks or cables, it is normally assumed that an electrical pulse (a step function or a square wave, etc.) is applied to one end of the network. The current at the other end of the cable or network can then be calculated with good precision.

When networks are exposed to nuclear-radiation pulses, the conditions are slightly different. It can be assumed with good reason that the nuclear pulse creates an electrical pulse in the target. However, the nuclear irradiation does not apply to a differential small section of the network or cable, but is effective over several

feet of the cable. Thus, a multitude of electrical transients is created. Each differential element of the exposed length of the cable creates its specific electrical transient. These transients are not equal. They will differ in signal shape and magnitude for each specific geometry of exposure. Further, each single differential electrical pulse is transmitted over the cable in accordance with the rules of network theory, i.e., the pulse is reflected from non-matching sections of the circuit (such as open ends) and is transferred into damped oscillations because of the circuit parameters. These parameters change during irradiation. All the initial pulses and the reflected pulses are composed into a resultant signal at the end of the cable. Their relative phases, attenuation, and travel times have to be considered. In the most general case, the differential pulses per unit length of the cable are not the same for the different positions of exposed sections within the field of the nuclear-pulse source. Therefore, we cannot expect the resultant signal to be directly proportional to the distance from the nuclear source.

A mathematically tractable case has been chosen to prove the overall concept. This case corresponds to an experimental setup arranged so that the exposed section of the cable simultaneously receives a uniform irradiation. The length of this section is kept electrically short relative to the shortest transient wavelength created in the cable. Under this assumption the exposed cable can be represented by a coaxial capacitor. We call this case "the lumped-circuit approach."*

The nuclear-radiation burst changes the effective conductance and the electric properties of this capacitor in a transient fashion. It produces a spatial distribution of electric charges between the conductors of the exposed section of the cable. These charges manifest themselves in the form of an induced transient EMF between inner and outer conductor.*

The bias voltage is also acting in series with the induced EMF. This bias is applied to the cable either in a sense of opposite or equal sign with respect to the induced EMF pulse. In this case, "the lumped circuit" was chosen for the first approach of the problem because the mathematical treatment is facilitated by the assumption of uniform radiation and the availability of experimental data.[2] This corresponds precisely to the assumptions that were made. In these experiments, the electrically open-ended, coiled-up portion of the cable constitutes a "coaxial capacitor." An electrical charge is supplied to the capacitor by a battery of voltage V, which is connected to the inner and outer conductors of the cable through a series resistance of magnitude R, equal to the characteristic impedance Z_0 of the otherwise loss-less cable. Additional charge is introduced by incident nuclear particles which are carried by the radiation pulse into the capacitor, or are created by the nuclear interaction within the cable materials which results in ionization.

* We assume that the outer conductor is grounded and therefore neglects the effect of a possible unsymmetric EMF between ground and either one of the conductors.

B. Theoretical Model

The conversion of the radiation energy is described by a change in the capacitive and conductive properties of the materials in the coaxial capacitor, and by a charging of the capacitor with a corresponding formation of an impressed electromotive force e(t) upon it. That is, the irradiated portion of the cable becomes a transient battery of which the EMF and the internal impedance are both controlled by the radiation burst.

C. Validation of Approach

The validity of the "lumped-circuit" approach is based upon the following: 1) the time of wave propagation through the coiled-up portion of the cable is very short as compared to the duration of the radiation burst, i.e., the electrical length of the coiled-up cable is short as compared to the shortest wave-length in the transient spectrum which results from the burst; 2) the coiled-up portion of the cable is so compact that each incremental length is subject to the same dose-rate; 3) the experimental layout is such that the remaining straight cable is practically unaffected by the pulse of radiation.

D. Assumptions Required for Derivation

For mathematical tractability, a direct proportionality is assumed to exist between the radiation-burst shape and the transient parameters. This assumption does not reduce the generality of the approach since nothing is assumed about the nuclear, atomic, or molecular mechanism of the transient damage. The burst shape is taken as it is resolved by the detection instruments.* It shall be proportional to the following transient parameters: dynamic capacitance, dynamic conductance, and induced EMF. The dynamic capacitance may be either positive or negative, since there is a possibility of either an increase or decrease in total capacitance under radiation. The dynamic conductance is always assumed to be positive; and the induced EMF may be either positive or negative, relative to the bias voltage V and/or relative to the dynamic capacitance.

The shape of the radiation pulse is assumed to be:

$$p^n(t) = e^{-n\left[\frac{1}{at} + (at)^2\right]}$$

---

* We will see later that the open-ended cable as such can be used as a radiation detector; in this respect see also (1).

where n and α are certain constant form factors. Although the actual shape of the pulse is unknown, this deduction can be made on the basis that pulse-reactor processes are relaxation processes triggered by fission, and governed by the diffusion differential equation. The steep rise of a relaxation transient is described* by the term $e^{-\frac{n}{\alpha t}}$ while the decay, described by $e^{-n(\alpha t)^2}$, is typical of diffusion processes.

Burst created charge-density distribution in the space between the inner and outer conductors, may produce an effective increase in the original (static geometric) capacitance. This effect is analogous to the increase in capacitance of electron tubes from a cold state to the hot state. However, the transitory charge-density distributions may also produce an effective negative dynamic capacitance dependent upon the mobility distribution of the charge carriers and upon the polarity and magnitude of the bias voltage V.

E. Justification for the Assumption

It will be shown that the assumption is justified by the high degree of agreement between the theoretical and experimental voltage and current responses, and by the fact that: 1) a change in the material parameters is a change in the effective dielectric constant of the cable insulation, which, with the influenced charges produces a change in the capacitance; 2) the liberation of charged particles from nuclear bonds (ionization) leads to an increase in the conductivity of the material in question; and 3) the induced EMF stands for the influence of these charges on the inner and outer conductors of the cable.

F. Mathematical Formulation

The equivalent circuit resulting from the lumped-circuit formulation is shown in Figure 1, where the circuit to the left is considered as the only portion subjected to irradiation. The circuit parameters appearing in the diagram will have the following definitions:

$c(t) = C_o + C_1(t)$	Capacitance
$g(t)$	Conductance of the Insulation
$e(t)$	Nuclear EMF
V	Bias Battery Voltage
$Z_o = R$	Characteristic impedance of cable termination resistance
$i(t)$	Total current
t	Time
$u_c(t)$	Voltage on C(t)
$q_c(t)$	Charge on C(t)

*More generally one may use $e^{-\frac{n}{(\alpha t)^k}}$ where k is another form factor (In a strict solution of the differential equation $k = \frac{1}{2}$).

Observe that $C_1(t)$, which is the dynamic capacitance of the cable, may be either positive or negative; whereas C_o, the original static capacitance, is positive. $g(t)$ is positive, and $e(t)$ may be either positive or negative, relative to the polarity of V and/or to $g(t)$.
The following analytical conditions are true:

$$i_c(t) = \frac{dq_c}{dt} = c(t)\ \frac{d}{dt}(u_c) + u_c(t)\ \frac{dc}{dt} \tag{1}$$

$$i_g(t) = u_c\ g(t) \tag{2}$$

$$i(t) = i_c(t) + i_g(t) \tag{3}$$

$$u_c(t) = V + e(t) - Ri(t). \tag{4}$$

Solving these equations simultaneously for $i(t)$, we obtain

$$\left[Rc(t)\right]\frac{di}{dt} = i\left[1 + Rg(t) + R\frac{dc}{dt}\right] + \left[e(t) + V\right]\left[g(t) + \frac{dc}{dt}\right] + c(t)\frac{de}{dt}. \tag{5}$$

In accordance with the assumptions as outlined in section D, the burst shape $P^n(t)$ is introduced:

$$P^n(t) = e^{-n\left[\frac{1}{at} + (at)^2\right]}$$

$$g(t) = g_m\ P^n(t)$$

$$e(t) = e_m\ P^n(t) \tag{6}$$

$$c(t) = c_m\ P^n(t).$$

The radiation burst functions P^n are plotted in Figure 2 for $n = 1, 2, 3$; $x = at$ is normalized time. For comparison, an experimental radiation burst curve, obtained by E.G.&G.*[3] is shown in Figure 3 in normalized form, in order to give coincidence of the peaks and starting point at $x = 0$.

* Edgerton, Germeshausen, and Grier

The theoretical peak of $P^n(x)$ has a value of

$$\left[P^n(x) \right]_{max} = \left[0.151 \right]^n \text{ at } x = x_B = \sqrt[3]{0.5} \doteq 0.8$$

where

( )

$$\frac{dP}{dx} = 0 \qquad \text{i.e.} \qquad \left(\frac{1}{x^2} - 2x \right) = 0 .$$

The width of the radiation pulse at half the pulse height, designated as half-height width, is denoted by T_n and is related with graphical accuracy to α by

$$T_1 = \frac{0.85}{\alpha} \qquad T_2 \doteq \frac{0.6}{\alpha} \qquad T_3 = \frac{0.45}{\alpha} .$$

(7')

G. Mathematical Discussion of Equation (5)

(a) Circuit time constant smaller than radiation pulse duration.

Several specializations of equation (5) have important physical significance. These are expressed as limiting cases of the circuit parameters in the following development.

The mathematical condition $R \to 0$ corresponds to the practical case where the peak time constant $RC(t)_{max} = \tau_{max} \ll T$ is much smaller than the radiation burst width. When in addition, the conductance $g(t) \ll \frac{1}{Z_0} = \frac{1}{R}$ remains always much less than the value of the characteristic admittance, i.e., $Rg(t) \ll 1$, then

under these conditions, equation (5) is reduced to:

$$i(t) \cong \left[e(t) + V\right]\left[g(t) + \frac{dc}{dt}\right] + c(t)\frac{de}{dt}$$

for

$$Rc(t) \ll T \quad \text{and} \quad Rg(t) \ll 1 .$$

(8)

The condition $Rg(t) \ll 1$ is essential. Otherwise for $Rg(t) \to 1$, we have the physical equivalent to an almost complete insulation breakdown of the dielectric, where the current is limited only by the termination resistance R, and not controlled by the conductance of the cable insulation.

(b) Circuit time constant of same order of magnitude or larger than radiation pulse duration:

Although the above specialization is of importance with relation to the final radiation resistivity of wires and cables, a solution of the general equation (5) is required, especially when the peak time constant of the circuit is of the same order of magnitude as the half-width of the radiation burst. i.e.

$$[Rc(t)]_{max} \approx T.$$

In practice, this will be the case for actual capacitors in the microfarad range rather than for lengths of coaxial cables normally used in radiation exposure experiments. The general solution of (5) is derived as follows

$$\frac{di}{dt} + \frac{1 + Rg(t) + R\frac{dc}{dt}}{Rc(t)}\, i(t) = \frac{1}{Rc(t)}\left\{\left[e(t) + V\right]\left[g(t) + \frac{dc}{dt}\right] + c(t)\frac{de}{dt}\right\}.$$

(9)

This is an equation in the form of

$$\frac{di}{dt} + f_o(t)\, i(t) = f_1(t)$$

which has (9')

$$e^{+\int f_o(t)\, dt}$$

as an integrating factor. This equation has an easily recognizable solution when one notes that

$$\frac{d}{dt}\left(e^{\int f_o(t)dt} i(t)\right) = e^{\int f_o(t)dt} \frac{di}{dt} + f_o(t)\, e^{\int f_o(t)dt}\, i(t)$$

or

$$e^{\int f_o(t)dt}\, i(t) = \int f_1(t) e^{\int f_o(t)dt} dt + K$$

whence (10)

$$i(t) = e^{-\int f_o(t)dt}\left[\int f_1(t) e^{\int f_o(t)dt} dt + K\right].$$

(10')

Now, the integration is carried out from t = 0 to t. Since we assume, though have not previously stated, that a virgin cable with insulation undamaged before the radiation pulse is the object of our consideration, then at

$$t = 0, \qquad g(0) = 0, \quad i(0) = 0 \quad \text{and hence } k = 0;$$

the solutions are

$$i(t) = e^{-\int_0^t f_0(t)dt} \left\{ \int_0^t f_1(t) e^{+\int_0^t f_0(t)dt} dt \right\} \tag{11}$$

where from equations (9) and (9')

$$f_0(t) = \frac{1}{Rc(t)} + \frac{q(t)}{c(t)} + \frac{1}{c} \cdot \frac{dc}{dt} \tag{11'}$$

$$f_1(t) = \frac{e(t) + V}{R} \left[\frac{q(t)}{c(t)} + \frac{1}{c} \frac{dc}{dt} \right] + \frac{1}{R} \frac{de}{dt} . \tag{11''}$$

H. Normalization

The introduction of the following normalization into equations (5) and (8) in connection with (6) greatly facilitates calculations. These normalizations are given below. The index 0 refers to static cable parameter, the index m to the maximum of the transient variable.

$$x = \alpha t \; ; \qquad \frac{d}{dt} = \alpha \frac{d}{dx}$$

$$\gamma_o = \frac{\alpha C_o}{gm} = \alpha \tau_{o,m} \; ; \qquad \gamma_m = \frac{\alpha c_m}{gm} = \alpha \tau_m$$

$$\frac{e_m}{V} = \lambda \; ; \quad \frac{1}{RC_o} = \beta_o \; ; \quad \frac{1}{Rc_m} = \beta_m \, . \tag{12}$$

Physically γ_o and γ_m represent the ratios of time constants to burst duration involving the static and dynamic capacitance. The specialization for $|Rc(t)| \ll T$ represented by (8), with the substitutions from (12), results in

$$i(x) = \left[e_m P^n(x) + V \right] \left[g_m P^n(x) + \alpha c_m \frac{d}{dx} P^n(x) \right]$$

$$+ e_m \left[C_o + c_m P^n(x) \right] \alpha \frac{d}{dx} P^n(x)$$

and since

$$\frac{d}{dx} P^n(x) = \frac{d}{dx} e^{-n(\frac{1}{x} + x^2)} = P^n(x) \quad n\ (\tfrac{1}{x^2} - 2x)$$

we have

$$i(x) = e_m \left[P^n(x)\right]^2 \left[g_m + 2\, c_m n\ (\tfrac{1}{x^2} - 2x)\right]$$

$$+ V \cdot P^n(x) \left[g_m + \alpha c_m n(\tfrac{1}{x^2} - 2x)\right]$$

$$+ e_m P^n(x) \left[\alpha C_o n\ (\tfrac{1}{x^2} - 2x)\right]. \qquad (13)$$

For $|V| \gg e_m$ (13) reduces to

$$\frac{i(x)}{V g_m} = y(x) = P^n(x) \left[1 + \gamma_m n(\tfrac{1}{x^2} - 2x)\right]. \qquad (13')$$

This corresponds to the experimental case where large bias voltages are applied (large compared to the induced EMF, i.e., $|\lambda| \to 0$). The shapes of the corresponding normalized current responses, produced by a radiation burst of the form $P^1(x)$, are plotted in Figure 4. This figure shows quantitatively the influence of γ_m on the location of the current response peak. One may note that the peak response occurs before the burst peak in full conformance with the experimental response curves (See Figures 12 and 14). Another specialization of equation (13)

is the case for V = 0 (i.e., no battery bias voltage); this case results in

$$\frac{i(x)}{e_m g_m} = y(x) = \left[P(x)\right]^2\left[\, 1 + 2\gamma_m n(\tfrac{1}{x^2} - 2x)\right.$$

$$\left. + P^n(x)\left[\, \gamma_o n(\tfrac{1}{x^2} - 2x)\right]. \right.$$

(13")

For n = 1 the shapes of the corresponding normalized current transient responses are plotted in Figures 5 and 6. for positive and negative dynamic capacitance. In both cases γ_o is much smaller than $|\gamma_m|$, i.e., the dynamic peak capacitance exceeds 15% (See equations 6 and 7) of the static capacitance. One sees by comparison of Figures 5 and 6 the influence of the sign of γ_m, which is also that of the dynamic capacitance. The location of the zero crossing of the response relative to the location of the radiation burst peak is different in both cases. Negative γ_m makes the response zero crossing occur before the radiation burst peak. This fact is a typical characteristic of the transient response for V = 0, obtained experimentally (See Figure 14). Apparently no experimental evidence exists so far for positive γ_m. Under the above condition V = 0 (See Evaluation examples 2 and 3).

The more general solution of the specialization $|c(t)| \ll T$ applies when the e_m of the induced EMF and the battery bias voltage V are of the same order of magnitude, i.e., $|\lambda| = |\frac{e_m}{V}| \approx |$.

In this case we have

$$\frac{i(x)}{Vg_m} = y(x) = \left[P^n(x)\right]\left\{\left[1 + \lambda P^n(x)\right] + n(\tfrac{1}{x^2} - 2x)\left[\gamma_m(1 + 2\lambda P^n(x)) + \gamma_o\lambda\right]\right\}. \qquad (13''')$$

The shapes of the corresponding normalized current response transients are plotted in Figure 7. The radiation burst shape is assumed with $P_1(x)$. The λ has been chosen with 6 and -6 respectively (i.e., $V' = [e(t)]_{max}$ and $V = -[e(t)]_{max}$).

The influence of the relative polarity of battery bias voltage is clearly seen by comparison of the two curves of Figure 7. One may note the similarity of the characteristics of the theoretical and the corresponding experimental curves (See Figure 14, and example 3 of the evaluation).

Thus, the consistent similarity of the characteristics of the experimental and theoretical response curves clearly shows that the specialization $|Rc(t)| \ll T$, and the relevant formulas (13'), (13''), and (13'''), are applicable for quantitative evaluation of observed transient nuclear radiation effects in terms of transient cable parameters (dynamic capacitance, dynamic conductance, induced EMF). In addition, the form factor n of the burst shape function can be deduced by a comparison of experimental with theoretical response curves (See evaluation procedure and example 2 of evaluation).

Returning to equation (11), (11'), and (11'') and using the normalizations (12) one obtains the solution of the general case as follows

$$f_o(x) = a \frac{1 + Rg_m P^n(x) \left[1 + \gamma_m n(\tfrac{1}{x^2} - 2x)\right]}{Rg_m \left[\gamma_o + \gamma_m P^n(x)\right]} \tag{14}$$

$$f_1(x) = a \frac{V}{R} \frac{P^n(x) \left[1 + \lambda P^n(x)\right] \left[1 + \gamma_m n(\tfrac{1}{x^2} - 2x)\right]}{\left[\gamma_o + \gamma_m P^n(x)\right]} . \tag{14'}$$

From which we obtain

$$\frac{i(t)}{Vg_m} = y(x) = \exp\left[-\int_o^x \frac{1 + Rg_m P^n(x) \left[1 + \gamma_m n(\tfrac{1}{x^2} - 2x)\right]}{Rg_m\left[\gamma_o + \gamma_m P^n(x)\right]} dx\right]$$

$$\left\{\int_o^x dx \cdot \left[\frac{P^n(x) \left[1 + \lambda P^n(x)\right] \left[1 + \gamma_m n(\tfrac{1}{x^2} - 2x)\right]}{Rg_m\left[\gamma_o + \gamma_m P^n(x)\right]}\right.\right.$$

$$\left.\left. \exp \int_o^x dx \frac{1 + Rg_m P^n(x) \left[1 + \gamma_m n(\tfrac{1}{x^2} - 2x)\right]}{Rg_m\left[\gamma_o + \gamma_m P^n(x)\right]} \right]\right\} . \tag{15}$$

This equation is the most general solution of the problem that defies an exact analytic evaluation in a closed format, which is required if $[Rc(t)]_{max} \approx T$. Because this case may arise in practice with either cable or electronic components of large capacitance, a graphical solution has been carried out with the following numerical values

$$[Rg(t)]_{max} \ll 1 \quad ; \qquad Rg_m\gamma_o = \alpha RC_o = \frac{\alpha}{\beta_o} = 0.5$$

$$\gamma_m = o \qquad\qquad n = 1$$

$$|\lambda| = \left|\frac{\gamma_m}{\gamma_o}\right| \to 0 \qquad (15')$$

$\lambda = 0$ is used because in many circuits large capacitances are employed in a charged-up condition with higher voltages applied to them (e.g., D.C. blocking capacitors, filters, etc.). The graphical evaluation is represented by Figure 8a and 8b, showing the various terms contributing to the integral and the resultant solution $y(x)$ (See Figure 7b). This evaluation proceeds as follows: A burst shape $P'(x)$ is assumed; equations (14) and (14') become with (15')

$$f_o(x) = \beta_o\left[1 + Rg_m P'(x)\right] = \beta_o\left[1 + Rg_m e^{-\frac{1}{x} - x^2}\right]$$

$$f_1(x) = \beta_o V P'(x) = \beta_o V e^{-\frac{1}{x} - x^2} \qquad (15'')$$

and (15) becomes

$$y(x) = e^{-\frac{\beta}{\alpha}\Omega} \int_0^x [1 + Rg_m P^1(x)]\, dx$$

$$\frac{\beta}{\alpha}\Omega \int_0^x \left[P^1(x)\, e^{\frac{\beta}{\alpha}\Omega \int [1 + Rg_m P^1(x)]\, dx} \right] dx \,. \tag{16}$$

The influence of the magnitude of Rg_m on the exponential term of equation (16) is given in Figure 8a. The approach

$$\int_0^x [1 + Rg_m P^1(x)]\, dx \doteq x$$

for

$$Rg_m \ll 10$$

is obviously permissible because

$$P^1(x) < 0.151 \,.$$

For $Rg_m > 10$, the term

$$\int_0^x [1 + Rg_m P^1(x)] dx$$

rises essentially in conformance to the dose curve $\Phi(x)$ of Figure 2 and finally approaches x.

Pursuing the case,

$$Rg_m \ll 10 \,,$$

equation (16) reduces to

$$y(x) \doteq 2\, e^{-2x}\left[\int_0^x e^{+2x}\; e^{-\frac{1}{x}-x^2}\, dx\right] \qquad (16')$$

for which the graphical solution appears in Figure 8b. For the numerical integration of $\Phi(x) = \int_0^x P'(x)dx$, Simpson's method was followed, while for the integration of $\int_0^x e^{2x}P'(x)dx$, the trapeze method was used. The resulting response curve $y(x)$ has been transplotted from the semilog coordinate system of Figure 8b to a linear coordinate system in Figure 9, scaled in amplitude for comparison with the original radiation burst shape. Attention is called to the characteristic occurrence of the current transient response peak following the radiation burst peak.

The graphical construction in Figure 8a and 8b reveals that other approximate solutions of equation (16) can be derived analytically for the following specializations

$$\frac{\beta_o}{\alpha} \gg 1 \qquad \text{and} \qquad Rg_m \ll 1 \;,$$

$$\frac{B_o}{\alpha} \ll 1 \qquad \text{and} \qquad Rg_m \ll 1 \;,$$

and all values of $\frac{\beta_o}{\alpha}$ where $Rg_m \gg 10$.

In the case $\frac{\beta_o}{\alpha} \gg 1$, i.e., $RC_o \ll T$ the integrand term $P(x)$ varies only slightly as compared to $e^{\frac{\beta_o}{\alpha}x}$ if $Rg_m \ll 1$.

Hence, $P'(x)$ can be removed from the integral in equation (16).

The obvious result is

$$y(x) = P'(x) \qquad (17)$$

which agrees with equation (13') for $\gamma_m = 0$.

This case is included in Figure 2. Equation 17 reflects the situation where one has a static time constant $RC_o \ll T$, smaller than the burst width, and a negligible dynamic capacitance, i.e., $c(t) = C_o = \text{const}$. Thus, the current is controlled by the conductance $g(t)$, the time dependence of which is directly proportional to the radiation burst shape function $P(x)$. This case regarding the direct measurement of the radiation burst shape is potentially important (Dose rate meter), and usually occurs with low impedance targets.

Conversely, in the case $\frac{\beta_o}{\alpha} \ll 1$ the analytical approximation for the solution of equation (16) follows from $e^{\frac{\beta_o}{\alpha} x} \approx 1$ in the interesting range $0 \leq x \leq 3$ for $Rg_m \ll 1$.

This yields in (16)

$$y(x) = \frac{\beta_o}{\alpha} e^{-\frac{\beta_o}{\alpha} x} \int_o^x P'(x)\, dx = \frac{\beta_o}{\alpha} e^{-\frac{\beta_o}{\alpha} x} \Phi(x). \qquad (18)$$

The corresponding current transient responses are given in Figure 10. The integrating action of the circuit with $RC_o \gg T$ permits the response peak to occur long after the radiation burst peak, with subsequent pulse stretching by simple exponential decay. Current response curves of this shape will be found in practice when large capacitors kept at higher voltage potential are being irradiated.

In the case where $Rg_m \gg 10$ the term $\int_o^x Rg_m P'(x)\, dx$ varies faster than x and can be much greater than x in the range of interest for $x \leq 3$.

Approximately, (16) is then

$$y(x) \doteq e^{-\frac{\beta_o}{\alpha}\left[x + \int_o^x P'(x)\, Rg_m dx\right]} \int_o^\infty \frac{\beta_o}{\alpha} P'(x)\, e^{+\frac{\beta_o}{\alpha}\int_o^x P'(x)\, Rg_m dx}\, dx$$

$$= \frac{e^{-\frac{\beta_o}{\alpha}x}}{Rg_m}\, e^{-\frac{1}{\gamma_o}\int_o^x P'(x)dx}\, e^{\frac{1}{\gamma_o}\int_o^x P'(x)dx} \quad ;$$

thus

$$y(x) \doteq \frac{e^{-\frac{\beta_o}{\alpha}x}}{Rg_m} .$$

Therefore,

$$i(x) = Vg_m y(x) = \frac{V}{R}\, e^{-\frac{\beta_o}{\alpha}x}$$

for

$$Rg_m \gg 10.$$

(19)

Equation (19) represents a spike-like transient current arising from a practically complete break-down of the insulation, long before the radiation burst has reached its peak. The peak amplitude $\frac{V}{R}$ of this current spike, is limited only by the termination resistance R.

I. Evaluation Procedures

In the preceding paragraph, the consistent conformance of the characteristics of theoretical and experimentally obtained current responses demonstrates the fundamental validity of the theoretical model.

The quantitative evaluation of these irradiation effects in terms of electrical circuit parameters, can be made, therefore, from this model. The evaluation is, mathematically, a matching of experimental curves with theoretical curves that correspond to the formulas set forth. The matching is done by taking k measurements on a response curve, thus establishing k equations to obtain a numerical solution for the k unknowns. Among the unknowns, there may be not only the electrical parameters, but also the nuclear radiation burst shape parameters n, α, or even the absolute time origin.

The following characteristics of the current response are instrumental in the evaluation procedure: 1) location of response peaks relative to the location of the radiation burst peak in an amplitude, time diagram; 2) location of amplitude crossings of the time axis relative to the location of the radiation burst peak; 3) the slope at such a zero crossing and/or the location of the maximum slope; 4) ratio of relative maximum and minimum, and their location on the time axis; and 5) absolute magnitude of current response peaks.

In the absence of an absolutely complete simultaneous record of the dose rate, certain characteristics of the radiation burst are instrumental in the evaluation, viz., 1) timing of the occurrence of the radiation burst peak (dose rate peak), and 2) half-height width T or some other suitable measure to be used for the duration of the radiation burst.

a) Evaluation procedure for large battery bias voltage for

$$|\lambda| \to 0 \qquad \text{i.e.,} \qquad |V| \gg e_m$$

follows from setting the derivative of (13') to zero which gives

$$\frac{dv}{dx} = p^n(x)\left\{n\left(\frac{1}{x_1^2} - 2x_1\right)\left[1 + \gamma_m n\left(\frac{1}{x_1^2} - 2x_1\right)\right] - 2\gamma_m n\left(\frac{1}{x_1^3} + 1\right)\right\} = 0.$$

This yields the relation between the location x_1 of the peak of the response and

$$\gamma_m = \frac{\left(\frac{1}{x_1^2} - 2x_1\right)}{2\left(\frac{1}{x_1^3} + 1\right) - n\left(\frac{1}{x_1^2} - 2x_1\right)^2} = \frac{1 - 2x_1^3}{2\left(\frac{1}{x_1} + x_1^2\right) - n\left(\frac{1}{x_1} - 2x_1^2\right)^2} \qquad (20)$$

The evaluation of γ_m from the relative location of the response peak x_1 is most practical if zero crossings are buried in noise, or are so flat that their location cannot be precisely measured; otherwise, γ_m could be readily found from the zero crossing at x_o in (13') by

$$\gamma_m = \frac{1}{n(2x_o - \frac{1}{x_o^2})} . \qquad (20')$$

Both x_1 and x_o are measured in fractions, or multiples of the time of occurrence of the radiation burst peak normalized to $x_B = 0.8$ (See Equation 7). Substitution of γ_m into (13') at x_1 gives the peak value $y(x_1)$. From the measured peak current $i(x_1)$ and the known bias voltage V,

$$y_m = \frac{i(x_1)}{Vy(x_1)} \qquad (20'')$$

is found, so that, in turn from γ_m in accordance with (12)

$$c_m = \frac{g_m \gamma_m}{a} = \frac{\gamma_m}{a} \frac{i(x_1)}{Vy(x_1)} \qquad (20''')$$

can be obtained.

a is given by the known burst half-height width. In the case of a burst shape, conforming for example to $P^1(x)$, we have

$$a \doteq \frac{0.85}{T_1} .$$

Now all parameters are numerically evaluated.

b) Evaluation procedure for zero battery bias voltage, i.e., $V = 0$ follows from (13''). Several methods are practicable.

1) For a known burst shape, two equations for the two unknowns γ_m and γ_0, can be derived by using normalized peak and zero crossing time of the response. The current peak amplitude gives, with the found γ_m and γ_0, the third equation for the unknown e_m :

$$\left(\frac{dy}{dx}\right)_{x_1} = 0 \qquad y(x_0) = 0 \tag{21}$$

$$\gamma_m \left[4n^2\left(\frac{1}{x^2} - 2x_1\right)^2 - 4n\left(\frac{1}{x^3} + 1\right)\right] p^n(x_1) + \gamma_0 \left[n^2\left(\frac{1}{x_1^2} - 2x_1\right)^2 - 2n\left(\frac{1}{x_1^3} + 1\right)\right]$$

$$= -p^n(x_1)\, 2n \left(\frac{1}{x^2} - 2x\right)$$

$$\gamma_m \left[2n \left(\frac{1}{x_0^2} - 2x_0\right)\right] p^n(x_0) - \gamma_0 \left[n \left(\frac{1}{x_0^2} - 2x_0\right)\right] = -p^n(x_0).$$

(21')

Here, as above, x_1 and x_0 are the observed peak and zero crossing locations, respectively, measured in fractions or multiples of the time

of occurrence of the radiation burst peak normalized to $x_B = 0.8$. The actual peak conductance and dynamic peak capacitance are then readily obtained from (12) e.g., the ratio $\frac{\tau_m}{\tau_o} = \frac{C_m}{C_o}$ gives C_m since C_o is known, and g_m follows from τ_o with $g_m = \frac{aC_o}{\tau_o}$, where, as before, $a = \frac{0.85}{t}$ for a burst shape described by $P'(x)$.

The magnitude of e_m is then found by substituting the values for τ_m and τ_o into the equation (13") at x_1, thus, forming the value $y(x_1)$. With the measured peak current $i(x_1)$ and the already known g_m, one finds the factor e_m of the induced EMF

$$e_m = \frac{i(x_1)}{g_m y(x_1)} .$$

2) For an unknown burst shape parameter n, three equations for the three unknowns n, τ_m, τ_o can be derived by using normalized times of two peaks and one zero crossing. Similarly, as before, the current peak response yields with the n, τ_m, τ_o a fourth equation for the unknown e_m. This method is used in the numerical example given in the following paragraph.

c) Evaluation procedure for $V \neq 0$ and unknown $\lambda = \frac{e_m}{V}$

For a known radiation burst shape, three equations for τ_m, τ_o, λ can be established using normalized times of two peaks and one zero crossing, analogous to a and b above.

d) Evaluation procedure of records without simultaneous reference timing and dosimetry.

This problem can be solved as indicated below:

In principle, the transient current response versus recorded time t', is sufficient to solve for both transient electrical cable parameters,

as well as the radiation burst shape parameters. The current responses obtained with the zero bias voltage are best suited for this purpose because of their many significant characteristics. There are the well distinguished maxima, minima, slopes, and zero crossings.

If in practice, recording time count $t' = t + \delta$ is started with the activation of the mechanical reactor control mechanism, then δ accounts for the time delay between this mechanical activation and the actual start of the fission process, from which the evaluation reference time t is counted. The unknown values of the six parameters e_m, c_m, g_m, n, α, δ could then be solved for by forming with the relation (13'') six equations corresponding to the following measured characteristics of the current response:

Recorded time of zero crossings: t_o' ; $i(t_o') = 0$.

Slope angle φ in the zero crossing, i.e., $\left(\frac{di}{dt'}\right)_{t=t_o} = \tan \varphi_o$.

Recorded time of maximum and minimum t_1', t_2'

and associated current amplitudes i_1, i_2.

Recorded time for half maximum and half minimum amplitudes t_3', t_4'.

It is obvious that the numerical solutions will be very tedious. However, they will give value to experimental data which have been obtained without concurrent reference time scaling dosimetry, or where the dosimeter performance was doubtful. Therefore, it is possible to exchange experimental simplicity for analytical difficulty in the evaluation. To avoid this however, it is strongly emphasized that the reference time is obtained from a dose-rate meter.

In connection with the use of a dose-rate meter for reference time indication, the case of $\tau_o \ll \tau_m \ll 1$ for $|V| \ll e_m$

becomes extremely important. Equation (13") reduces under this condition to

$$y(x) \doteq \left[p^n(x)\right]^2$$

which has its peak at $x_B \doteq 0{\cdot}8$, but has a width that is narrower

than that of the actual radiation burst $P^n(x)$. Inferring that a dose rate meter has an equivalent electrical circuit similar to Figure 1 with

$\tau_o \ll \tau_m \ll 1$, then , the half-height width of the output

current response from the dose rate meter would be narrower than the half-height width of the actual burst shape; i.e., the recorded rate meter readings were not directly proportional to the actual radiation burst but were proportional to its square. Thus, the normalized half-height width appears equal to 0.6, instead 0.85.

J. Examples For Numerical Evaluation

1. Recorded Burst 12 (response labeled (22)) Figure 14

   Battery bias voltage V=225 volts

   Distance from source .97 feet (25 cm)

   Radiation burst half-height width T=70 microseconds

   Burst peak recorded at 15 mm from origin of the time scale used in Figure 14

   Voltage response peak at 11.5 mm from the origin of time record with 3m V on 75 ohms, i.e.

$$i_1 = 4.10^{-3} \text{ amp.}$$

Applicable formulae: (13') and $P^n(x) = e^{-n(\frac{1}{x} + x^2)}$

then

$$y(x) = P^n(x)\left[1 + n\gamma_m(\tfrac{1}{x^2} - 2x)\right] \cong \frac{i(t)}{Vg_m}$$

and equation (20)

$$\gamma_m = \frac{\frac{1}{x^2} - 2x_1}{2(\frac{1}{x^3} + 1) - n(\frac{1}{x^2} - 2x_1)^2}$$

Noting that the burst peak occurs at

$$x_B = at = 0{\cdot}8$$

and $\quad 15mm : 11.5mm = 0.8 : x_1$,

the burst peak occurs at normalized time

$$x_1 = \frac{11.5}{15}\ 0.8 = 0.61 \quad .$$

Consequently, we obtain

$$\gamma_m = \frac{2.66 - 1.22}{2(4.4 + 1) - n(2.66 - 1.22)^2} = \frac{1.44}{10.8 - 2.08n} \equiv \frac{ac_m}{g_m}$$

$$\frac{1}{[g(t)]_{max}} = r_{min} = y(x_1)\frac{225\ [6.6]^n}{4.10^{-3}} \quad (\Omega)$$

$$C_{1\ max} = c_m[P(0.8)]^n = [\gamma_m(n)]\ \frac{T}{[r_{min}(n)]\ [\Delta x(n)]} \ .$$

The evaluation results in the following

TABLE 1

n	1	2	3
γ_m	0.165	0.217	0.31
$y\ (0.61)$	$\frac{1.025}{6.6}$	$\frac{1.12}{(6.6)^2}$	$\frac{1.33}{(6.6)^3}$
($M\Omega$) r_{min} Note (1)	5.75	6.25	7.5
Δx	0.85	0.6	0.45
($\mu\mu F$) $C_{1\ max}$	+2.36	+4	+6.5

NOTE: (1) Δx is the half-height width (in normalized time) of $P^n(x)$ the radiation burst shape function. $C_{1\ max}$ the maximum dynamic capacitance $r_{min} = \frac{1}{[g(t)]_{max}}$ the minimum insulation resistance.

The normal static capacitance of the RG-59/U cable used in the experiment is listed with 21 micro-microfarad per foot, i.e., the 28' irradiated cable has a virgin capacitance $C_0 = 590\ \mu\mu F$. The results show that the nuclear irradiation burst produced a maximum transient change of capacitance of about + 1 %. Hence, relative to the virgin transconductance value of 10^{-9} mhos per meter for cables of this type at radio frequencies, the radiation burst produced about a sixteen-fold transient increase of the transconductance.

Example 2:

Recorded Burst 8 (response 18, Fig 14)

V = 0 (no battery in the circuit)

Distance from source .97 feet (25cm)

Radiation burst half-width T = 70 microseconds

Recorded voltage response characteristics:

Location of	Units (graph paper)	Voltage amplitude on 75 ohm terminating
Burst peak	12	
Response minimum	9.6 (second peak)	1.3 m V
Response zero crossing	7.5	
Response Maximum	6 (first peak)	.71 m V

Applicable formula (13")

$$\frac{i(t)}{e_m g_m} = y(x) = [P^n(x)]^2 \left[1 + 2\gamma_m n \left(\frac{1}{x^2} - 2x\right)\right] + n\gamma_o P^n(x) \left[\frac{1}{x^2} - 2x\right].$$

In normalized time,

$x_1 = \frac{6.0}{12} 0.8 = 0.4$ Location of first peak

$x_o = \frac{7.5}{12} 0.8 = 0.5$ Location of zero crossing

$x_2 = \frac{9.6}{12} 0.8 = 0.64$ second peak

$$\frac{1}{x_1^2} - 2x_1 = 5.37 \; ; \quad \frac{1}{x_2^2} - 2x_2 = 1.15 \; ; \quad p^n(0.4) = \left(\frac{0.4}{6.6}\right)^n$$

$$\frac{1}{x_1^3} + 1 = 16.6 \; ; \quad \frac{1}{x_1^3} + 1 = 4.82 \; ; \quad p^n(0.64) = \left(\frac{0.9}{6.6}\right)^n$$

$$\frac{1}{x_0^2} - 2x_0 = 3 \; ; \qquad p^n(0.5) = \left(\frac{0.63}{6.6}\right)^n$$

at

$$x_1 \text{ and } x_2 \qquad \frac{dy}{dx} = 0$$

yields

$$\left(\frac{dy}{dx}\right)_{1,2} = p^n(x) \left\{ p^n(x) 2n\left(\frac{1}{x^2} - 2x\right) - 2n\left(\frac{1}{x^3} + 1\right) \left[2\gamma_m p^n(x) + \gamma_o\right] \right.$$

$$\left. + n^2\left(\frac{1}{x^2} - 2x\right) \left[4\gamma_m p^n(x) + \gamma_o\right] \right\}_{x_1 x_2} = 0.$$

One obtains from the first peak,

$$0 = [0.06]^n \, 10.74 + \gamma_o \, (29n - 33.2) + [0.06]^n \gamma_m (116n - 66.4);$$

from the second peak,

$$0 = [0.136]^n \, 2.3 + \gamma_o (1.33n - 9.64) + [0.136]^n \, \gamma_m (5.32n - 19.28);$$

and from the zero crossing,

$$0 = [0.096]^n [1 + 6 n\gamma_m] + 3n\gamma_o .$$

The above can be brought into the form from the first peak,

$$0 = [0.06]^n + \gamma_o (2.7n - 3.06) + [0.06]^n [10.8n - 6.18] \gamma_m$$

from zero crossing,

$$0 = [0.096]^n + \gamma_o 3n + [0.096]^n 6n\gamma_m$$

from second peak,

$$0 = [0.136]^n + \gamma_o(0.58n - 4.2) + [0.136]^n [2.31n - 5.2] \gamma_m$$

representing three equations for the unknowns n; γ_m; and γ_o.

The occurrence of exponentials of n in these three equations makes it difficult to arrive at a direct solution. Hence, an approximate solution is presented which was arrived at by finding through graphical trial a value of n which produces a coincidence of two of the three equations. Toward this end, n is tried as being equal to 1, 2, and 3, and the relations $\gamma_o = \gamma_o(\gamma_m)$ are plotted graphically, representing straight lines.

Namely for $n = 1$

$$\gamma_o = + [0.06]^1 [3.3 + 15.4\gamma_m] = + 0.925 [0.214 + \gamma_m]$$

$$\gamma_o = - [0.096]^1 [0.33 + 2\gamma_m] = - 1.92 [0.166 + \gamma_m]$$

$$\gamma_o = + [0.136]^1 [0.276 - 1.37\gamma_m] = + 0.182 [0.2 - \gamma_m]$$

for $n = 2$

$$\gamma_o = - [0.06]^2 [0.416 + 6.43\gamma_m] = - 0.0232 [0.065 + \gamma_m]$$

$$\gamma_o = - [0.096]^2 [0.166 + 2\gamma_m] = -0.0184 [0.083 + \gamma_m$$

$$\gamma_o = + [0.136]^2 [0.33 - 0.58\gamma_m] = + 0.0108 [0.57 - \gamma_m]$$

for $n = 3$

$$\gamma_o = -[0.06]^3 [0.196 + 5.1\gamma_m] = -10^{-3}\, 1.07\, [0.0386 + \gamma_m]$$

$$\gamma_o = -[0.096]^3 [0.111 + 2\gamma_m] = -10^{-3}\, 1.76\, [0.055 + \gamma_m]$$

$$\gamma_o = +[0.136]^3 [0.46 + 0.7\gamma_m] = +10^{-3}\, 1.75\, [0.65 + \gamma_m].$$

A comparative inspection of the relations for $n = 1$, shows that because of the sign conditions no coincidence exists. Hence, only the relations $\gamma_o = \gamma_o(\gamma_m)$ for $n = 2$ and $n = 3$ have been plotted in Figure 11.

One comes closest to coincidence for $n = 2$ as the plot demonstrates. Thus, the burst shape parameter n is approximately equal to 2, and the normalized half-height width is with ($7'$) equal to 0.6.

From the plot, the values for γ_o and γ_m are found to be

$$\gamma_m = \frac{\alpha C_m}{g_m} = -0.107 \qquad \gamma_o = \frac{\alpha C_o}{g_m} = +0.075 \quad .$$

The capacitance of the RG-59/U cable is listed with 21 micro-microfarads per foot. Thus, the $28'$ tested have a capacitance of

$$C_o = 590\ \mu\mu F.$$

From γ_o , as above, T_2 for experiment (70 μsec) and

$$\alpha = \frac{[\Delta x]_{n=2}}{T_2} = \frac{0.6}{70.10^{-6}} = 0.85.10^{-4} \text{ sec}^{-1}.$$

It follows then that

$$g_m = \frac{(0.85.10^4)\ (590.10^{-12})}{0.075} = 6.7 \times 10^{-5}\ \Omega^{-1}$$

$$[g_m(t)]_{max} = \frac{1}{r_{min}} = g_m[p^2(x)]_{max} = g_m(0.151)^2 = 1.53 \times 10^{-6}\ \Omega^{-1}$$

and ,therefore,

$$\underline{\underline{r_{min} \doteq 0.65\ M\Omega}}$$

On the other hand

$$\frac{c_m}{C_o} = \frac{\gamma_m}{\gamma_o} = -\frac{0.107}{0.075} = -1.425$$

so that,

$$\frac{[c_1(t)]_{max}}{C_o} = \frac{c_m(0.151)^2}{C_o} = -0.037 \text{ i.e., } [c_1]_{max} = (-3.7\ ^o/_o) \text{ of } C_o.$$

The value of e_m follows by substituting the γ_m , γ_o in equation (13'')

$$i_1 = \frac{0.71.10^{-3}}{75} = 0.95 \times 10^{-5} = 9.5 \text{ μamp}$$

$$y(x_1) = [0.06]^4 [1 - 2 (0.107).2(5.37)]$$

$$+ [0.06]^2 [2(0.075) (5.37)]$$

$$= [0.06]^2 \{0.8 - 1.3 (0.0036)\}$$

$$= 2.9 \times (10^{-3}) \equiv \frac{i_1}{e_m g_m}$$

$$e_m = \frac{i_1}{g_m 2.9(10^{-3})} = \frac{9.5.10^{-6}}{(6.7.10^{-5})(2.9.10^{-3})} \doteq 50 \text{ Volt}$$

$$[e(t)]_{max} = e_m(0.151)^2 = 50 (0.151)^2 = 1.14 \text{ Volt.}$$

The conclusions drawn from the above results are: 1) the underlying nuclear radiation burst shape is closely approximated by a function

$$p^2(x) = e^{-2[\frac{i}{dt} + (\alpha t)^2]}$$

where

$$\alpha \doteq 8.5 \times 10^{-9} \text{ sec}^{-1} \quad .$$

2) The radiation burst produced a relative maximum transient change of capacitance of -3.7%, and brought the transconductance to a peak of about 1.6×10^{-7} mhos per meter (approximately a 160-fold peak increase from a typical normal 10^{-9} mhos/meter at RF). 3) The nuclear irradiation caused the creation of a transient electrical charge distribution in the insulation space, effecting a transient potential difference between inner and outer conductor which reached a peak of about one volt.

Example 3.

In this example, the records from burst 13 and 3, and subsequently burst 10 and 12 [response curves labeled (17) and (20); (21) and (22)] are analyzed in a comparative manner on the basis of the numerical results of examples 1 and 2. First, response (17) was obtained with V = -46.5 volts while response (20) needed V = +46.5 volts bias. Note, that the result in Example 2 was e_m = 50 volts, n = 2. In accordance with paragraph I(c) we use the result of Example 2, for which V = 0.

Therefore,

$$\frac{e_m}{V} = \lambda = \frac{50}{46.5} = -1.1$$

and

$$\frac{e_m}{V} = \lambda = \frac{50}{46.5} = +1.1$$

since

$$|\lambda| \ [P^2(x)]_{max} = |1.1| \ (0.151)^2 \ll 1 \quad .$$

The following approximation of (13''') is valid

$$\frac{i(x)}{g_m} = y(x) \doteq P^2(x) \left\{1 + 2\left(\frac{1}{x^2} - 2x\right)\left[\gamma_m + \lambda\gamma_o\right]\right\} . \tag{22}$$

Further, from Example 2, we obtain

$$\gamma_m = -0.107 \qquad \gamma_o = +0.075$$

hence, for

$$\lambda = -1.1 \qquad y(x) = P^2(x)\left\{1 - 2\left(\frac{1}{x^2} - 2x\right)(0.19)\right\}$$

and for

$$\lambda = +1.1 \qquad y(x) = P^2(x)\left\{1 - 2\left(\frac{1}{x^2} - 2x\right)(0.024)\right\}.$$

The influence of the sign of λ (i.e., polarity of V) is remarkable for

$$\lambda = -1.1 \qquad y(x) = P^2(x) - 0.19\,\frac{d}{dx}P^2(x)$$

and for

$$\lambda = +1.1 \qquad y(x) = P^2(x) - 0.024\,\frac{d}{dx}P^2(x).$$

Thus, the differentiation action of the second term is roughly ten times more pronounced for $\lambda = -1.1$ than for $\lambda = +1.1$ in full conformance to the character of the shape of the responses (17) and (20). The zero crossings in normalized time are obtained from $y(x_o) = 0$ at approximately $x_o = 0.22$ for $\lambda = +1.1$ and $x_o = 0.53$ (for $\lambda = -1.1$) before burst peak time. Hence, it is definitely established that response (17) represents the situation where induced nuclear EMF and bias voltage are of opposite polarity, while response (20) reflects the existence of equal polarity of nuclear EMF and bias voltage. What is more important in both cases is that the dynamic capacitance represented by γ_m, was negative but larger than γ_o. Therefore, in spite of the polarity change of V, the peak of responses(17) and (20) are recorded with the same polarity (recorded positive).

The subsequent experimental increase in bias voltage of the same polarity for the shots which led to response (21) and (22),made the dynamic capacitance change sign, i.e., γ_m positive, while at the same time $\lambda \to 0$ eliminates the influence of γ_o. For these cases, the approximate equation (22) becomes equivalent to equation (13'). Thus, with a positive γ_m, the response peaks are now recorded as being negative, even though the polarity of V remained unchanged going from (20) to (21) to (22). Essentially the same result would have been obtained if (13'') would have been used directly and solved for λ, γ_m, and γ_o in accordance with paragraph 1(c).

CONCLUSIONS

The discussed model has proved to be phenomenologically consistent with the experimental evidence. It is capable of quantifying electrical transient effects produced by nuclear bursts in transmission lines, and electrical components in terms of their transient electrical parameters. It is now possible to correlate consistently the natural electrical parameters of the cable with their radiation produced transients. The method permits one to differentiate between dynamic capacitance, dynamic transconductance, and induced EMF. Further, the comparison between theoretical and experimental transient responses has proven the initial assumption of direct proportionality between radiation burst shape and variation of electrical parameters. This radiation burst shape can be closely approximated by a function of the type

$$p^n(\alpha t) = e^{-n\left[\frac{1}{(\alpha t)^\kappa} + (\alpha t)^2\right]}$$

where

$$\alpha \doteq 8.5 \times 10^3 \text{ sec}^{-1}$$

under the given experimental circumstances.

The magnitude of the peak dynamic capacitance of the irradiated RG-59/U cable is only a few percent of the virgin capacitance of the cable. This dynamic capacitance is negative if zero or low bias battery voltages are being applied to the cable. For battery bias voltage larger than 50 volts, the dynamic capacitance is positive. The change of sign of the dynamic capacitance with increasing bias voltage of fixed polarity manifests itself by the inversion of the current response peak from recorded positive to recorded negative. The peak transconductance reaches values around 16×10^{-9} mhos per meter with large bias voltages applied to the cable. In the latter case, the output current response is in effect produced by an induced transient EMF of about 1 Volt peak.

The comparison of experimental circumstances under which an induced EMF and a dynamic capacitance are observed, versus other experimental circumstances in which only a complex impedance change is observed, suggests the phenomena similarly encountered in diodes. There, the velocity distribution of the electrons emitted from the cathode influences the potential distribution, especially at zero or low external bias voltages where a potential valley is created that prevents slower electrons from reaching the other electrode. Geometry and material both enter into the shape of this potential distribution which manifests itself as a thermionic EMF between the electrodes. A similar mechanism is suggested for the induced EMF and the negative dynamic capacitance, with the irradiated inner and outer conductor acting as electron sources. Geometry, and observed polarity of the induced EMF, should in this case be correlated, and further experimental work should be conducted to uncover such a correlation in different types of cables and other electronic components.

It has been further demonstrated that the time constants of the circuit, including target, cable, and terminations, play an important role. If the time constant of the target is small (low impedance targets), then for proper termination cable effects become negligible. On the other hand, it becomes difficult to separate target effects from cable and termination effects, if the time constants are of the same order of magnitude. These effects show up in terms of a differentiation or integration of the original radiation pulse shape. Thus, in the first case (differentiation), the response peaks occur before the burst peak, while in the second case (integration), they occur after the burst peak.

ACKNOWLEDGEMENT

It is a pleasure to acknowledge the assistance given by my associates at USAERADL in the development of the theoretical model for the explanation of observed nuclear radiation transient effects on cables; and the idea of the application of network theory to the case of transient nuclear damage introduced by Dr. P. R. Arendt who has also actively participated in the preparation of this report.

The author wishes to thank Dr. H. P. Bruemmer of Materials Branch, who gave us some insight into the nuclear-material aspects of the problem; Mr. Powell Reynolds, who helped immensely in the numerical and graphical evaluation of the resultant formulas; and the Boeing Company and Mr. H. W. Wicklein of this company for the courtesy to use their experimental data as cited under (2) in the literature index referenced below and the Figures 12, 13, and 14. The author also wishes to thank Mrs. Lillian Sacher and Mrs. Betty O'Connor, Institute for Exploratory Research, for their editorial assistance.

REFERENCES

(1) P. R. Arendt, "Comparison of Transient Effects Obtained with Different Nuclear Pulses," USASRDL Technical Report 2160, Nov. 1960; this report contains a bibliography of other reports and papers from USAERADL on the subject of transient nuclear damage. For a general literature survey see the "Accession Lists of the Radiation Effects Information Center of the Battelle Memorial Institute."

(2) H. W. Wicklein, "Transient Radiation Effects in Coaxial Cables Due to Gamma-Neutron Pulses," The Boeing Company, Doc. D2-90172, 1962, submitted for presentation at the Summer Meeting of the AIEE, Denver, Colorado, June 17-22, 1962, and for publication in the AIEE Transactions, also Sec. G. of Contributions to the State-of-the-Art of Transient Radiation Effects in Electronics Parts and Materials, The Boeing Company, Doc. D2-9878-3, 1962.

(3) Edgerton, Germeshausen, and Grier, Inc., "A Study of Radiation Effects on Electronic Devices," Signal Corps Contract Nr. DA36-039 SC-78171, DA Proj. No. 3-19-01-701, EG&G Report No. B-2000.

Fig. 1. Equivalent Circuit:

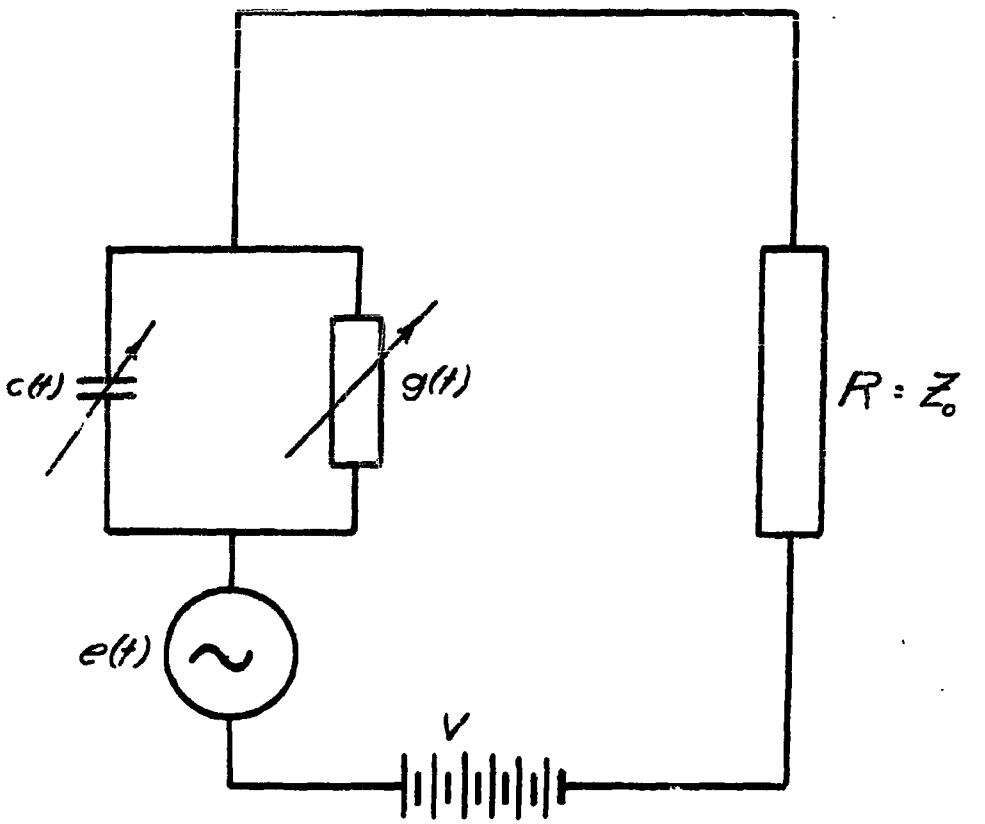

$c(t) = C_o + c_1(t)$ . . . . . .Capacitance

$c_1(t)$ . . . . . .Dynamic capacitance

$g(t)$ . . . . . .Conductance of the Insulation

$e(t)$. . . . . .Nuclear EMF

V. . . . . .Battery Bias Voltage

$R = Z_o$. . . . . .Characteristic Impedance

$i(t)$. . . . . .Total Current

t. . . . . .Time

$\mu_c(t)$ . . . . . .Voltage on c(t)

NOTE: e(t) may deduct or add to V, dependent on relative polarity.

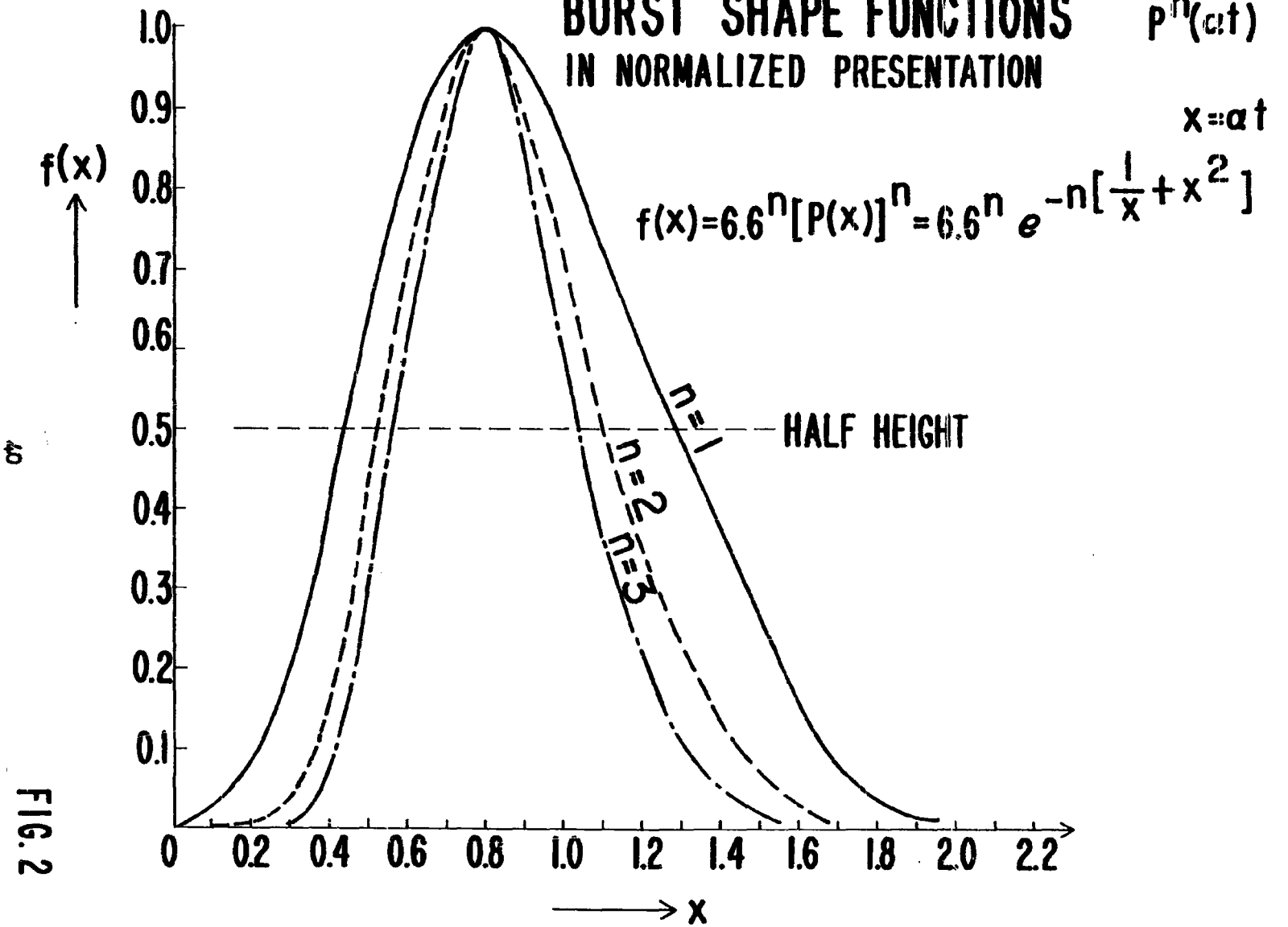
BURST SHAPE FUNCTIONS $P^n(\alpha t)$
IN NORMALIZED PRESENTATION
$x=\alpha t$
$f(x)=6.6^n[P(x)]^n=6.6^n\, e^{-n[\frac{1}{x}+x^2]}$
f(x)
1.0
0.9
0.8
0.7
0.6
0.5
0.4
0.3
0.2
0.1
HALF HEIGHT
n=1
n=2
n=3
0
0.2
0.4
0.6
0.8
1.0
1.2
1.4
1.6
1.8
2.0
2.2
x

FIG. 2

DOSE RATE SHOT 7 GODIVA

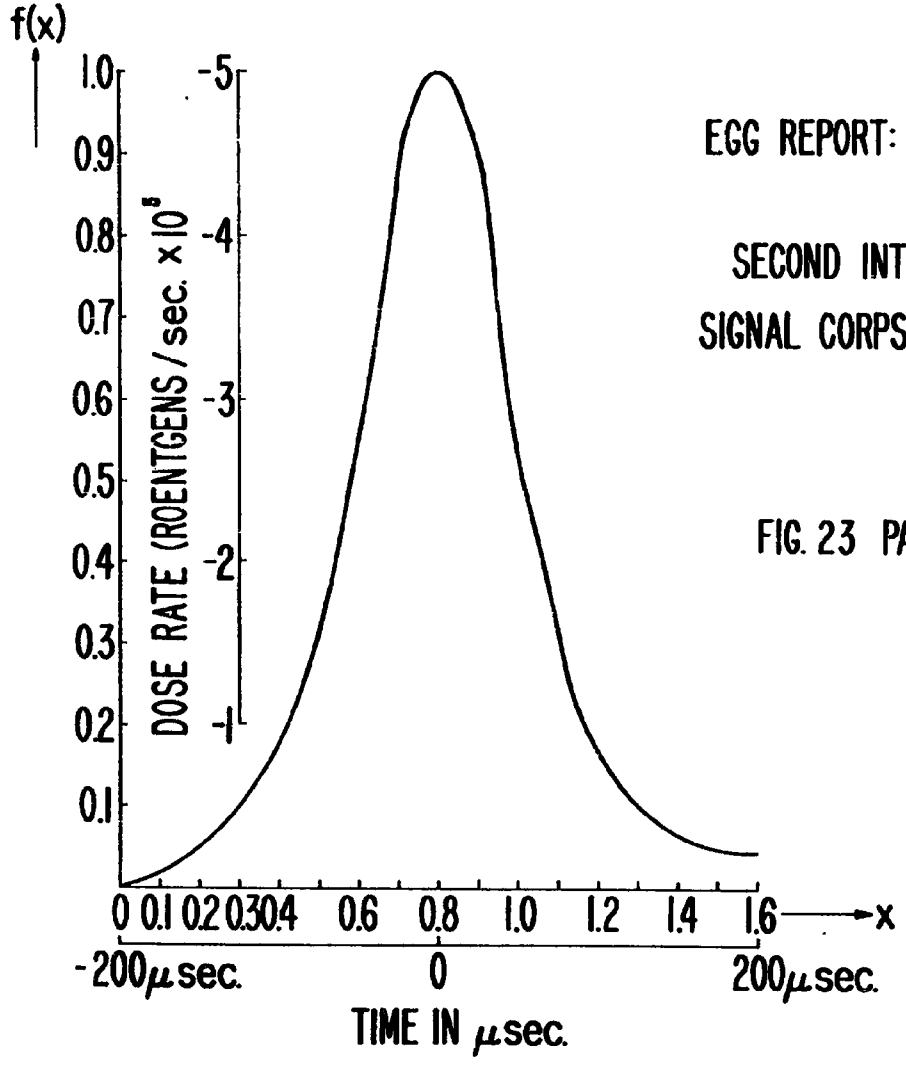

EGG REPORT: A STUDY OF RADIATION EFFECTS
ON ELECTRONIC DEVICES

SECOND INTERIM REPORT: 1 SEPT. 1959 - 30 NOV. 59

SIGNAL CORPS. CONTRACT NO. DA-36-039 SC 78171
DA PROJ. NO. 3-19-01-701
EG AND G REPORT NO. B-2000

FIG. 23 PAGE 52 (NORMALIZED)

FIG. 3

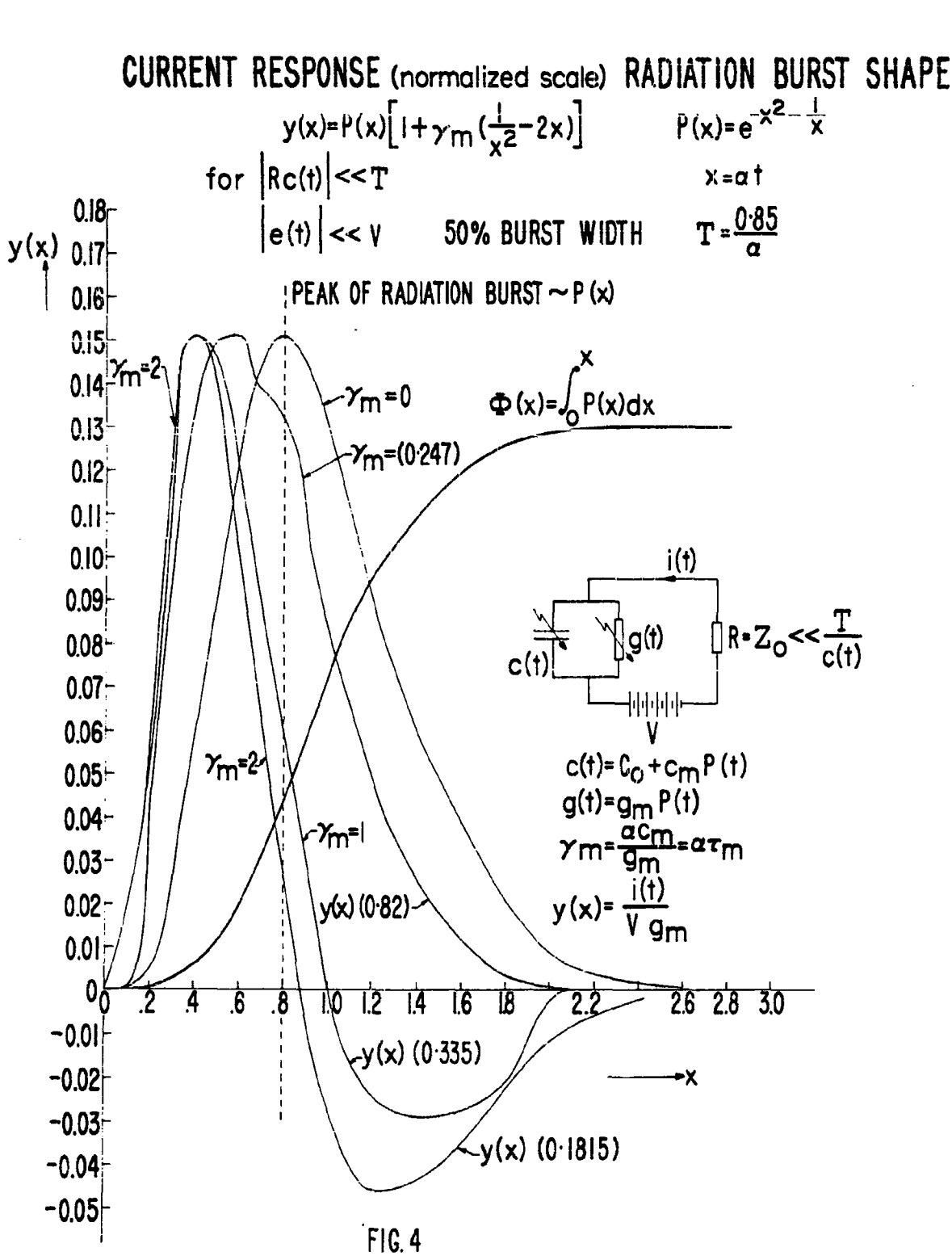
CURRENT RESPONSE (normalized scale) RADIATION BURST SHAPE
$y(x)=P(x)\left[1+\gamma_m\left(\frac{1}{x^2}-2x\right)\right]$
$P(x)=e^{-x^2-\frac{1}{x}}$
for $|Rc(t)|<<T$
$x=\alpha t$
$|e(t)|<<V$
50% BURST WIDTH
$T=\frac{0.85}{\alpha}$
PEAK OF RADIATION BURST ~ P(x)
y(x)
$\gamma_m=2$
$\gamma_m=0$
$\gamma_m=(0.247)$
$\gamma_m=1$
$\gamma_m=2$
$\Phi(x)=\int_0^x P(x)dx$
i(t)
c(t)
g(t)
$R=Z_0<<\frac{T}{c(t)}$
V
$c(t)=C_0+c_m P(t)$
$g(t)=g_m P(t)$
$\gamma_m=\frac{\alpha c_m}{g_m}=\alpha\tau_m$
$y(x)=\frac{i(t)}{V g_m}$
y(x) (0.82)
y(x) (0.335)
y(x) (0.1815)
x
0.18
0.17
0.16
0.15
0.14
0.13
0.12
0.11
0.10
0.09
0.08
0.07
0.06
0.05
0.04
0.03
0.02
0.01
0
-0.01
-0.02
-0.03
-0.04
-0.05
0
.2
.4
.6
.8
1.0
1.2
1.4
1.6
1.8
2.2
2.6
2.8
3.0

FIG. 4

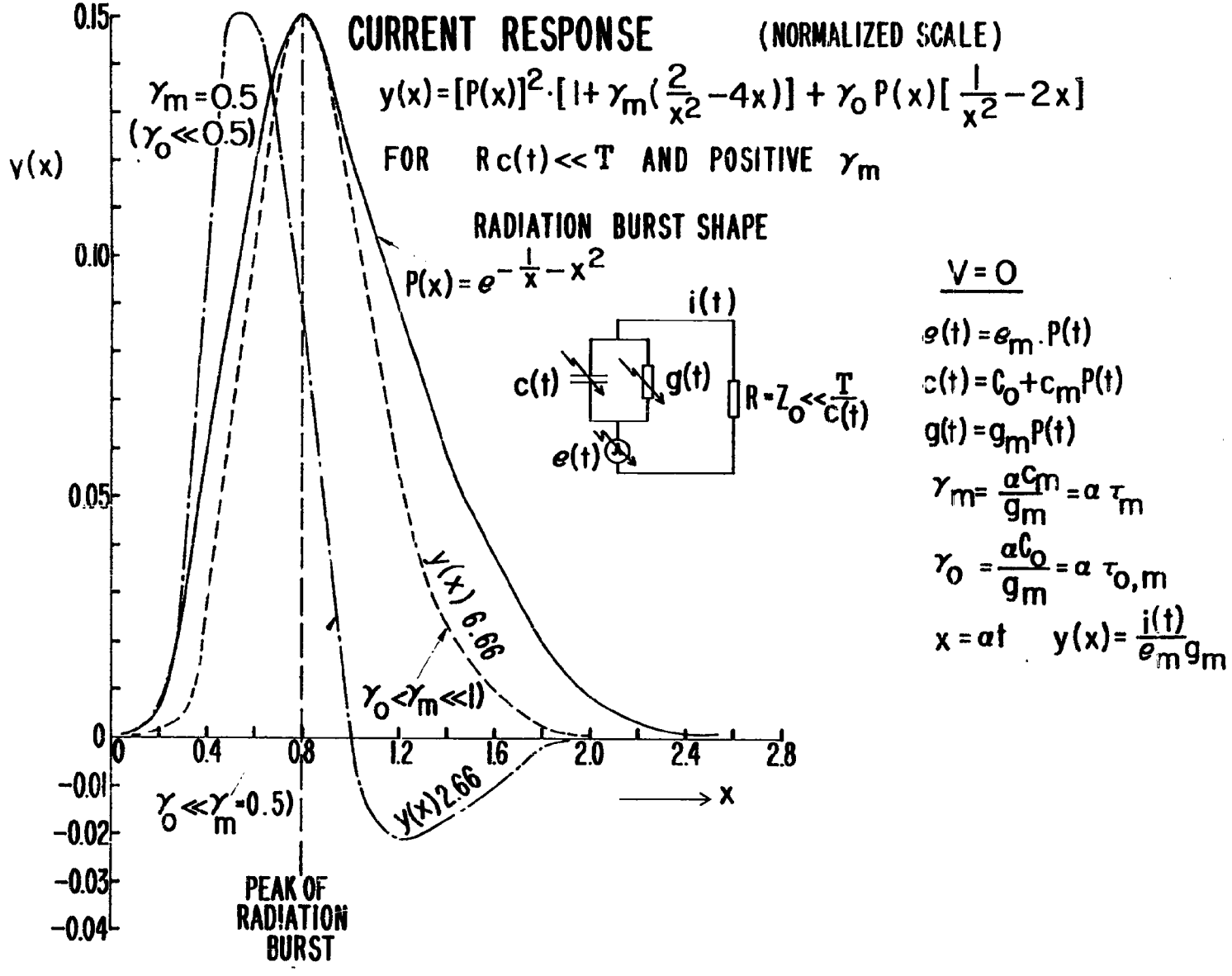
CURRENT RESPONSE (NORMALIZED SCALE)
$y(x)=[P(x)]^2\cdot[1+\gamma_m(\frac{2}{x^2}-4x)]+\gamma_0 P(x)[\frac{1}{x^2}-2x]$
FOR $Rc(t)\ll T$ AND POSITIVE γ_m
RADIATION BURST SHAPE
$P(x)=e^{-\frac{1}{x}-x^2}$
$\gamma_m=0.5$
$(\gamma_0\ll 0.5)$
$\gamma_0\ll\gamma_m=0.5)$
$\gamma_0<\gamma_m\ll 1)$
y(x) 6.66
y(x) 2.66
v(x)
x
0.15
0.10
0.05
0
-0.01
-0.02
-0.03
-0.04
0
0.4
0.8
1.2
1.6
2.0
2.4
2.8
PEAK OF RADIATION BURST
i(t)
c(t)
g(t)
e(t)
$R=Z_0\ll\frac{T}{c(t)}$
V = 0
$e(t)=e_m\cdot P(t)$
$c(t)=C_0+c_m P(t)$
$g(t)=g_m P(t)$
$\gamma_m=\frac{\alpha C_m}{g_m}=\alpha\,\tau_m$
$\gamma_0=\frac{\alpha C_0}{g_m}=\alpha\,\tau_{0,m}$
$x=\alpha t \quad y(x)=\frac{i(t)}{e_m g_m}$

FIG. 5

CURRENT RESPONSE (normalized scale)

$$y(x)=\left[P(x)\right]^2\left[1+2\gamma_m\left(\frac{1}{x^2}-2x\right)\right]+\gamma_0 P(x)\cdot\left[\frac{1}{x^2}-2x\right]$$

for $V=0$ $|R\cdot C(t)|\ll T$ & NEGATIVE γ_m

$$\gamma_m=\frac{\alpha c_m}{g_m} \quad y(x)=\frac{i(x)}{e_m g_m} \quad P(x)=e^{-\frac{1}{x}-x^2} \quad x=\alpha t \quad \alpha=\frac{0.85}{T}$$

$$\gamma_0=\frac{\alpha C_0}{g_m}$$

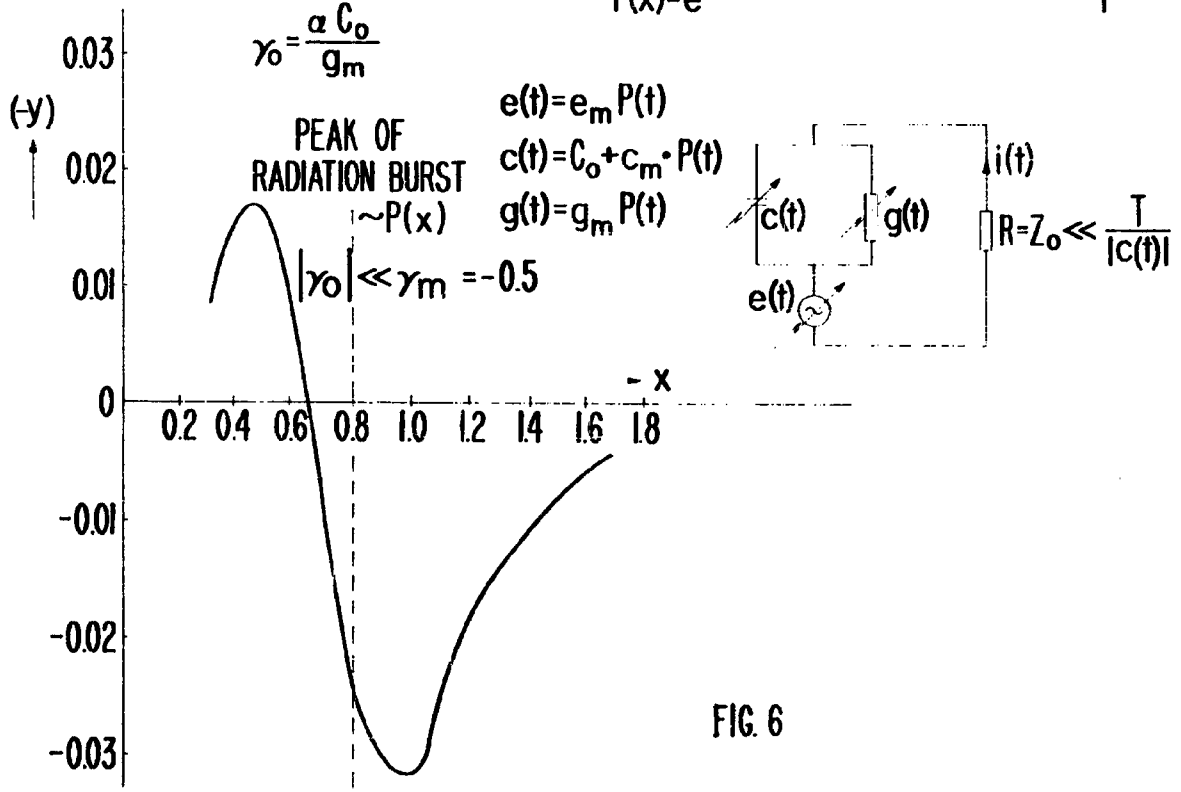

FIG. 6

CURRENT RESPONSE

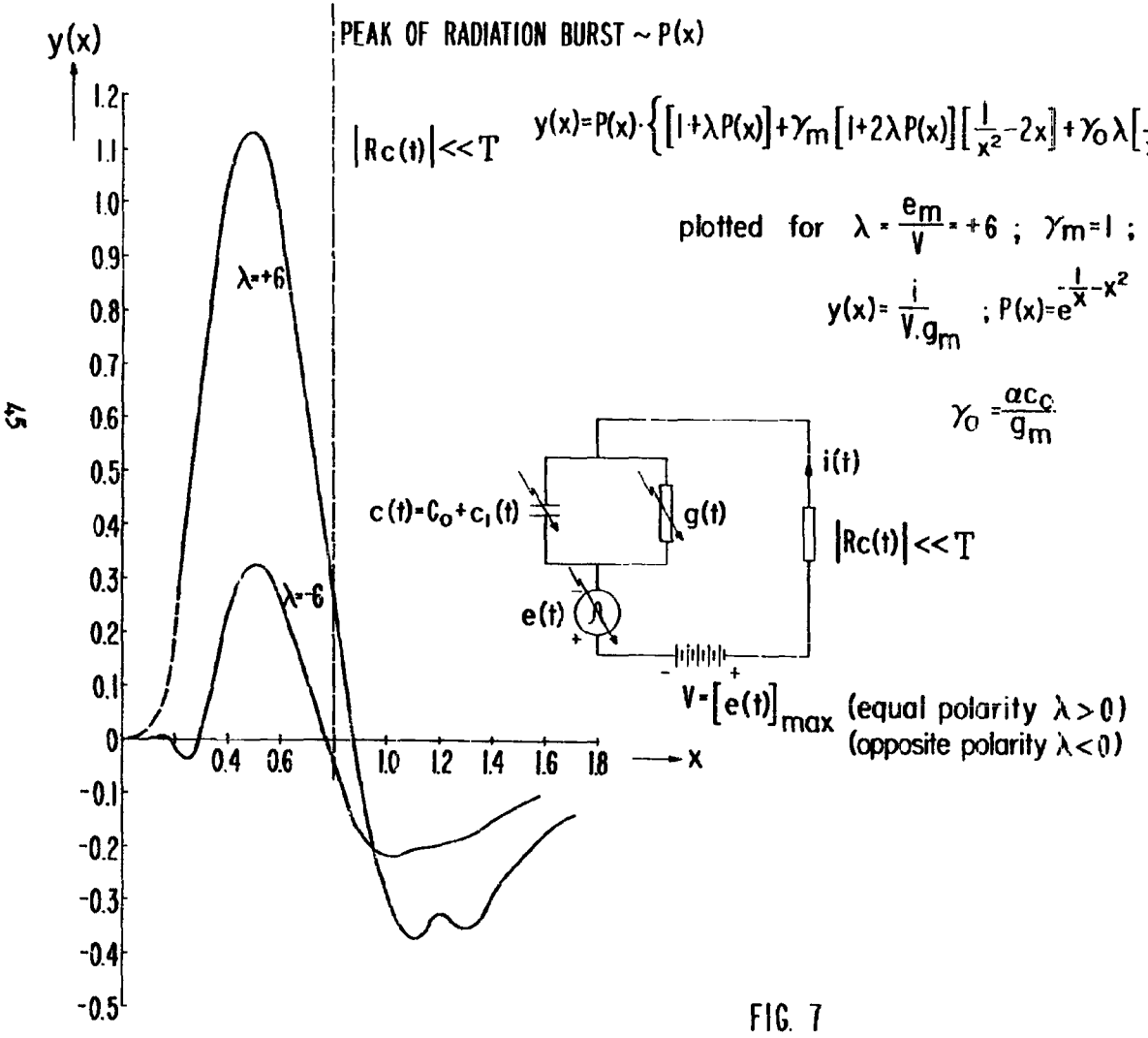

$|Rc(t)| \ll T$

$$y(x)=P(x)\cdot\left\{\left[1+\lambda P(x)\right]+\gamma_m\left[1+2\lambda P(x)\right]\left[\frac{1}{x^2}-2x\right]+\gamma_0\lambda\left[\frac{1}{x^2}-2x\right]\right\}$$

plotted for $\lambda=\frac{e_m}{V}=+6$; $\gamma_m=1$; $\gamma_0=\frac{1}{6}$ and $\lambda=\frac{e_m}{V}=-6$

$$y(x)=\frac{i}{V.g_m} \quad ; P(x)=e^{-\frac{1}{x}-x^2} \quad ; x=\alpha t \; ; \; \gamma_m=\frac{\alpha c_m}{g_m} \quad ; \alpha=\frac{0\cdot 85}{T}$$

$$\gamma_0=\frac{\alpha c_0}{g_m}$$

FIG. 7

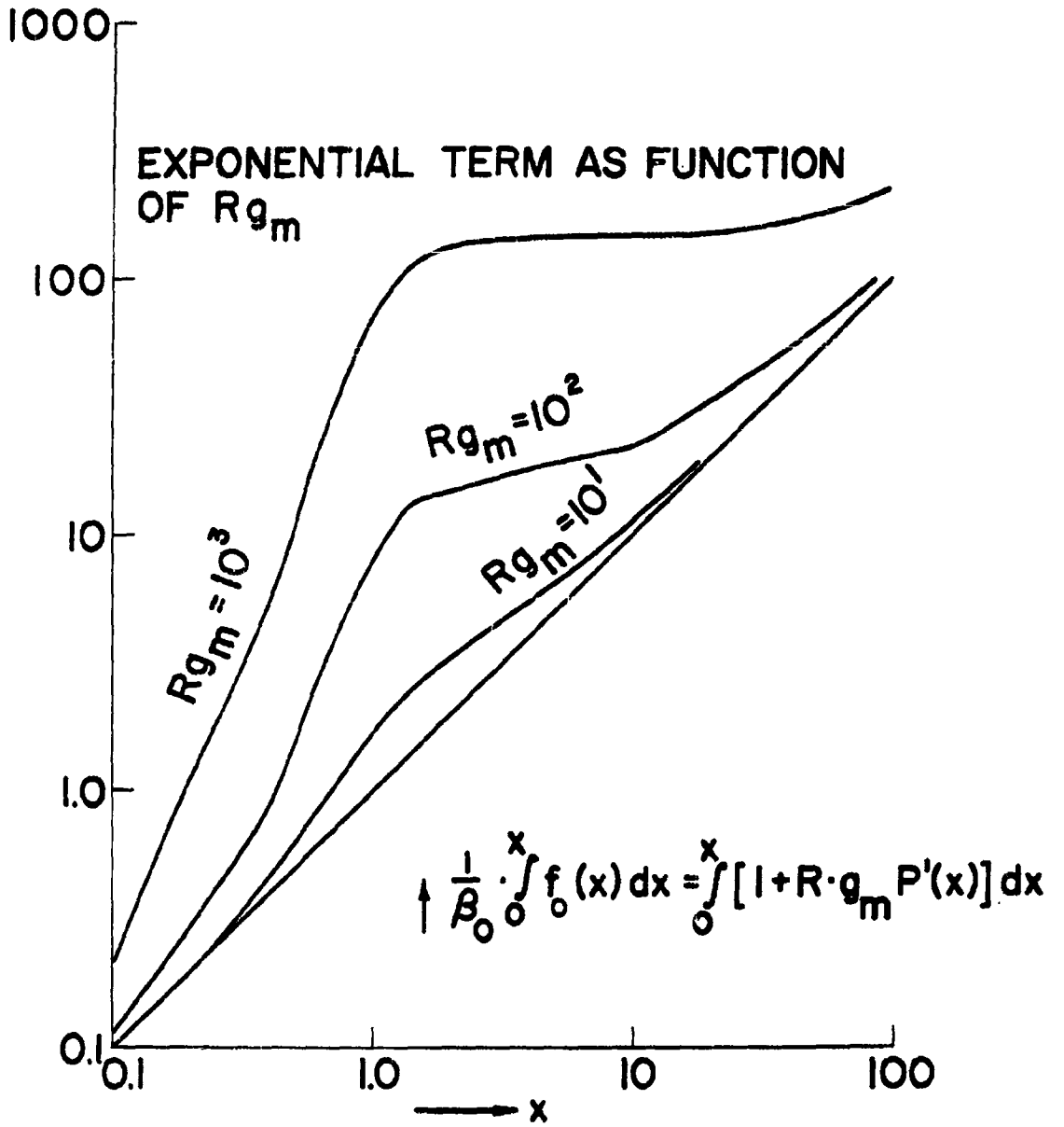
1000
100
10
1.0
0.1
EXPONENTIAL TERM AS FUNCTION
OF Rg_m
$Rg_m=10^3$
$Rg_m=10^2$
$Rg_m=10^1$
$\frac{1}{\beta_0}\int_0^x f_0(x)\,dx = \int_0^x [1+R\cdot g_m P'(x)]\,dx$
0.1
1.0
10
100
x

FIG. 8a

GRAPHICAL SOLUTION

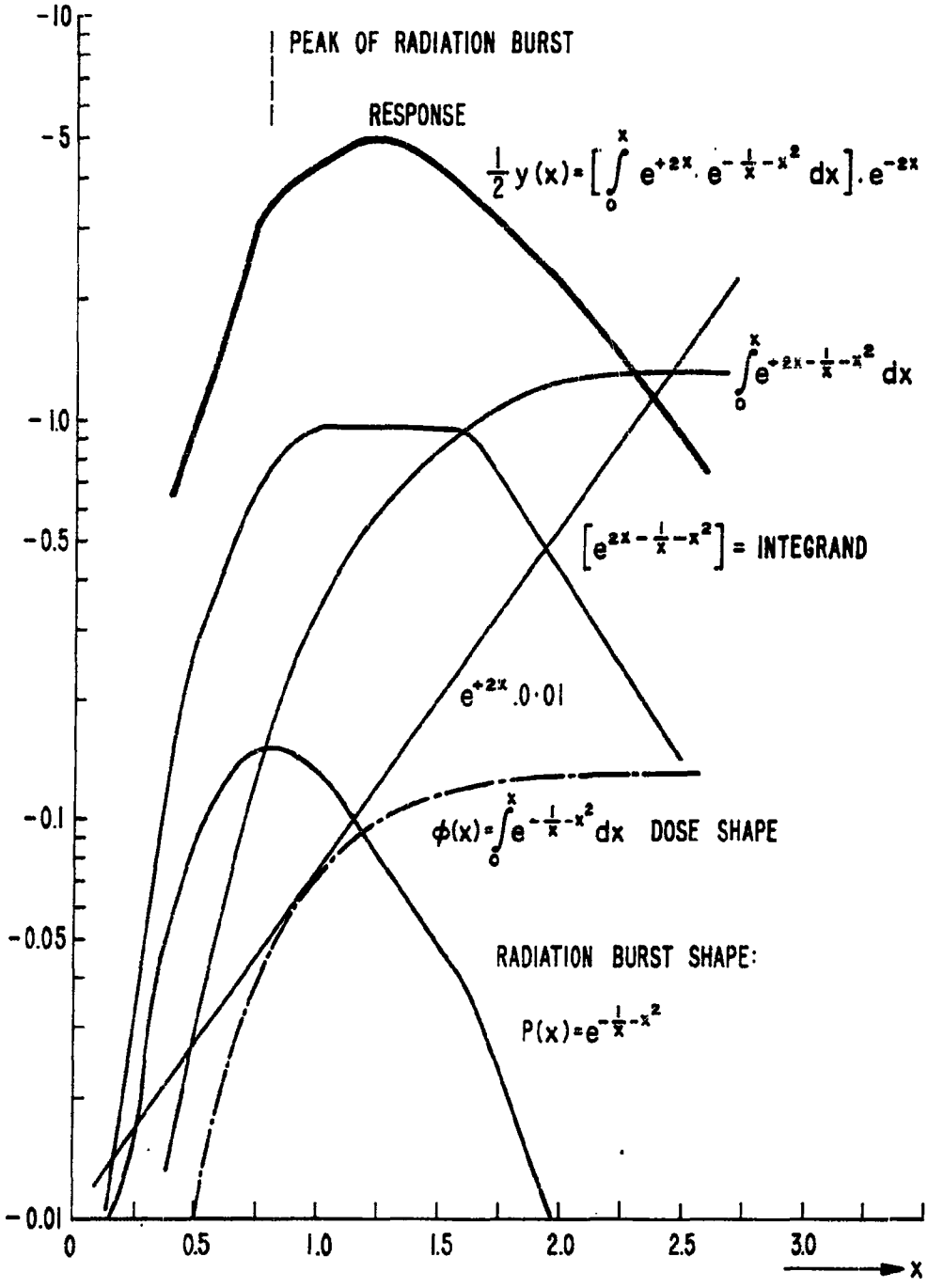

FIG. 8b

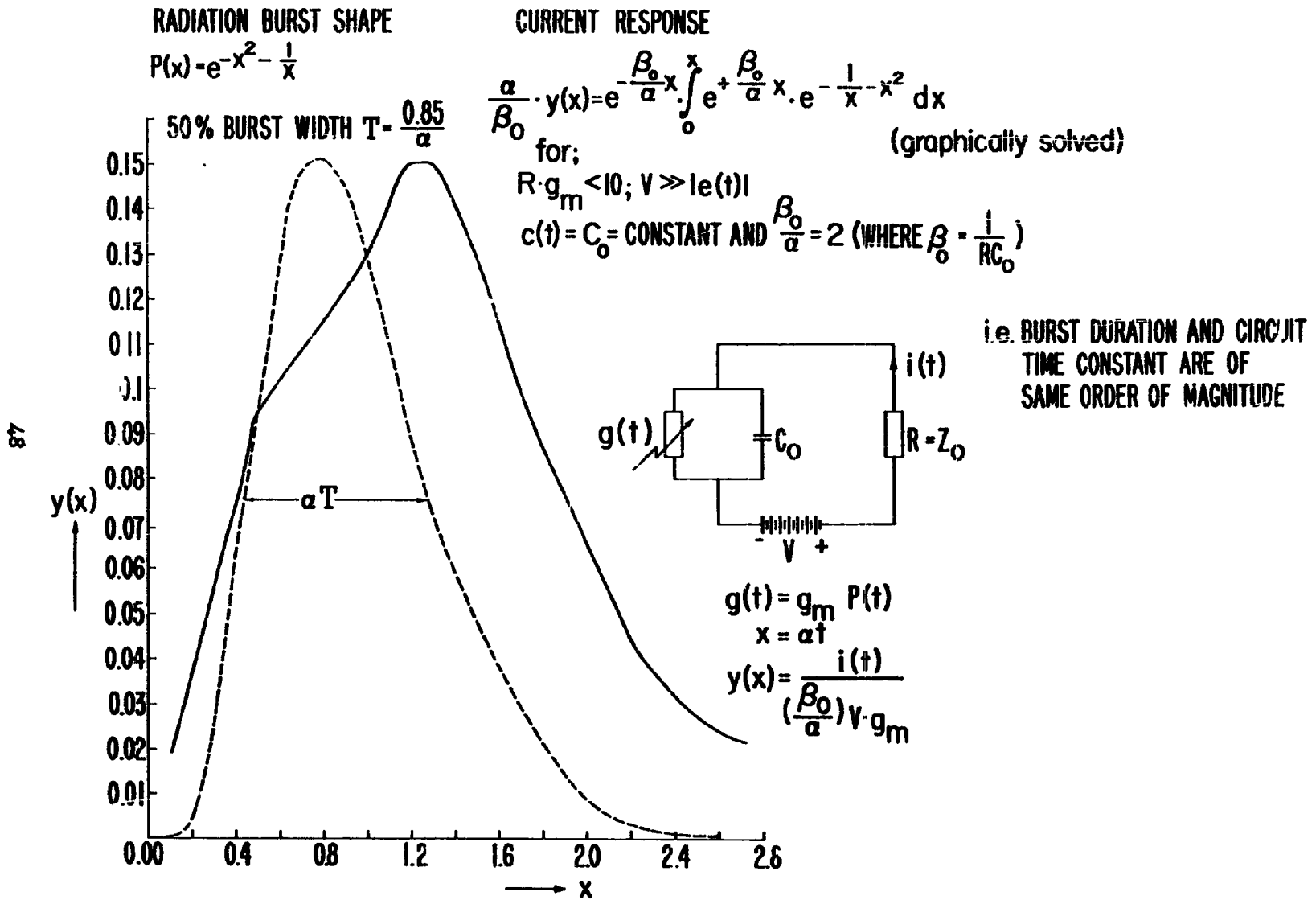
RADIATION BURST SHAPE
$P(x) = e^{-x^2} - \frac{1}{x}$
50% BURST WIDTH $T = \frac{0.85}{\alpha}$
CURRENT RESPONSE
$\frac{\alpha}{\beta_0} \cdot y(x) = e^{-\frac{\beta_0}{\alpha}x} \int_0^x e^{+\frac{\beta_0}{\alpha}x} \cdot e^{-\frac{1}{x}-x^2} dx$
(graphically solved)
for;
$R \cdot g_m < 10$; $V \gg |e(t)|$
$c(t) = C_0$ = CONSTANT AND $\frac{\beta_0}{\alpha} = 2$ (WHERE $\beta_0 = \frac{1}{RC_0}$)
i.e. BURST DURATION AND CIRCUIT TIME CONSTANT ARE OF SAME ORDER OF MAGNITUDE
i(t)
g(t)
C_0
$R = Z_0$
V
$g(t) = g_m P(t)$
$x = \alpha t$
$y(x) = \frac{i(t)}{(\frac{\beta_0}{\alpha}) V \cdot g_m}$
y(x)
αT
0.15
0.14
0.13
0.12
0.11
0.1
0.09
0.08
0.07
0.06
0.05
0.04
0.03
0.02
0.01
0.00
0.4
0.8
1.2
1.6
2.0
2.4
2.6
x

FIG. 9

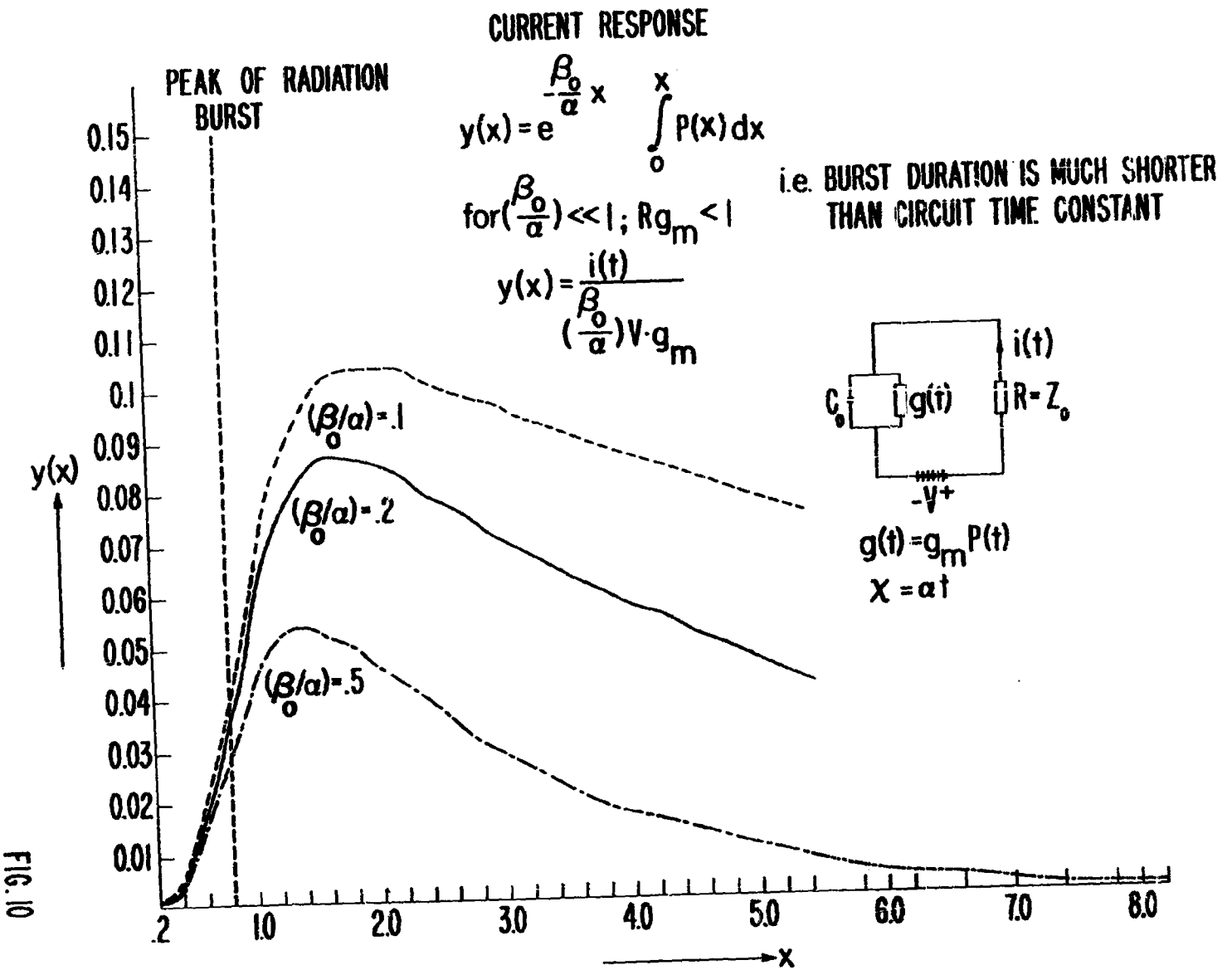
CURRENT RESPONSE
PEAK OF RADIATION BURST
$y(x) = e^{-\frac{\beta_0}{\alpha}x} \int_0^x P(x)\,dx$
for $(\frac{\beta_0}{\alpha}) \ll 1$; $Rg_m < 1$
$y(x) = \frac{i(t)}{(\frac{\beta_0}{\alpha})V \cdot g_m}$
i.e. BURST DURATION IS MUCH SHORTER THAN CIRCUIT TIME CONSTANT
C_0
g(t)
R = Z_0
i(t)
-V+
$g(t) = g_m P(t)$
$X = \alpha t$
y(x)
$(\beta_0/\alpha) = .1$
$(\beta_0/\alpha) = .2$
$(\beta_0/\alpha) = .5$
0.15
0.14
0.13
0.12
0.11
0.1
0.09
0.08
0.07
0.06
0.05
0.04
0.03
0.02
0.01
.2
1.0
2.0
3.0
4.0
5.0
6.0
7.0
8.0
X

FIG. 10

TRIAL SOLUTION FOR BURST SHAPE PARAMETER "n" OF $P^n(x)$

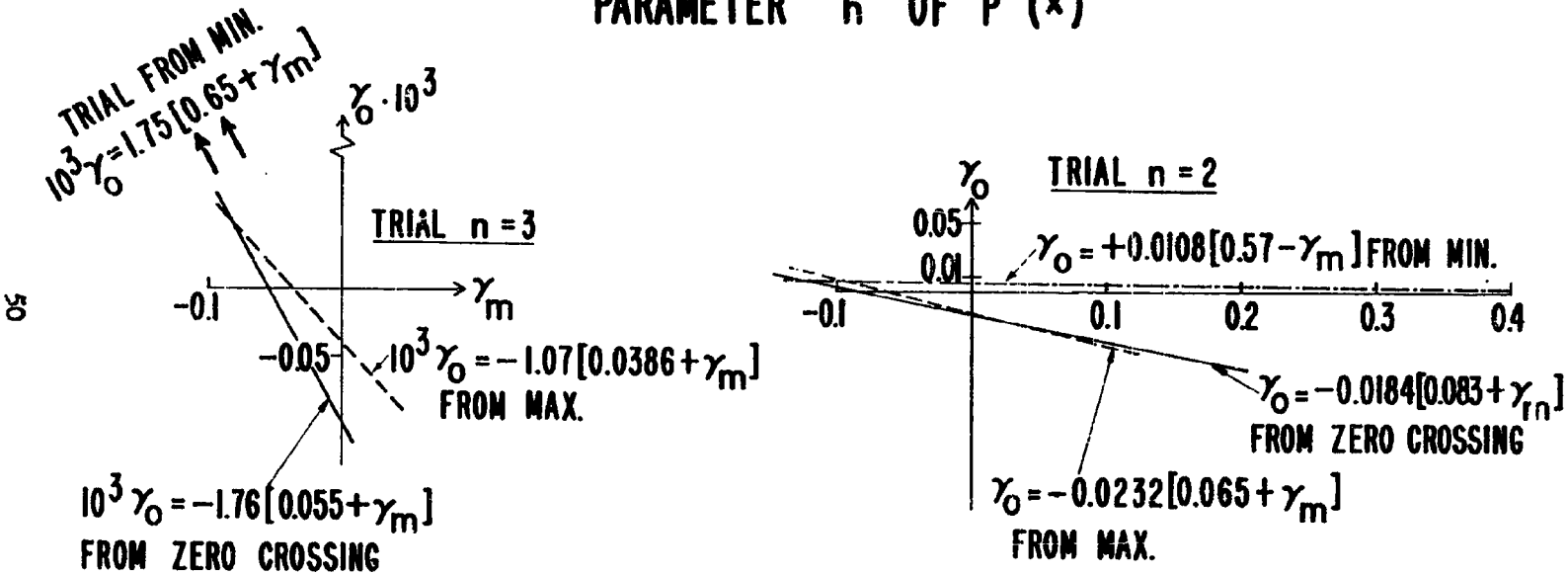

FIG. 11

TYPICAL DOSE AND RATE DEPENDENCE OF RADIATION-INDUCED CABLE SIGNALS
IN 28' UNIFORMLY-IRRADIATED UNBALANCED LENGTH OF RG-59B/U COAXIAL CABLE

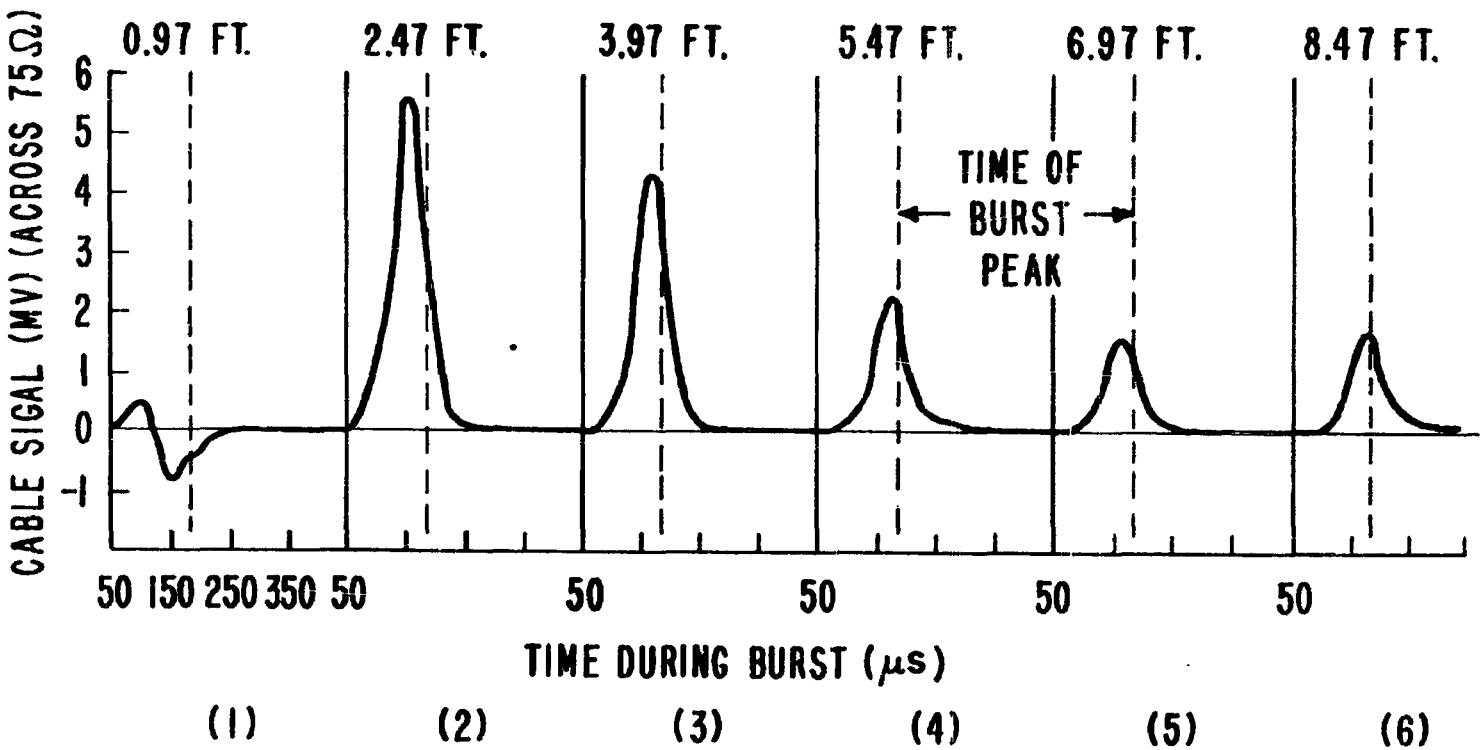

BURST 13; V=-46.5 VOLTS

FIG. 12

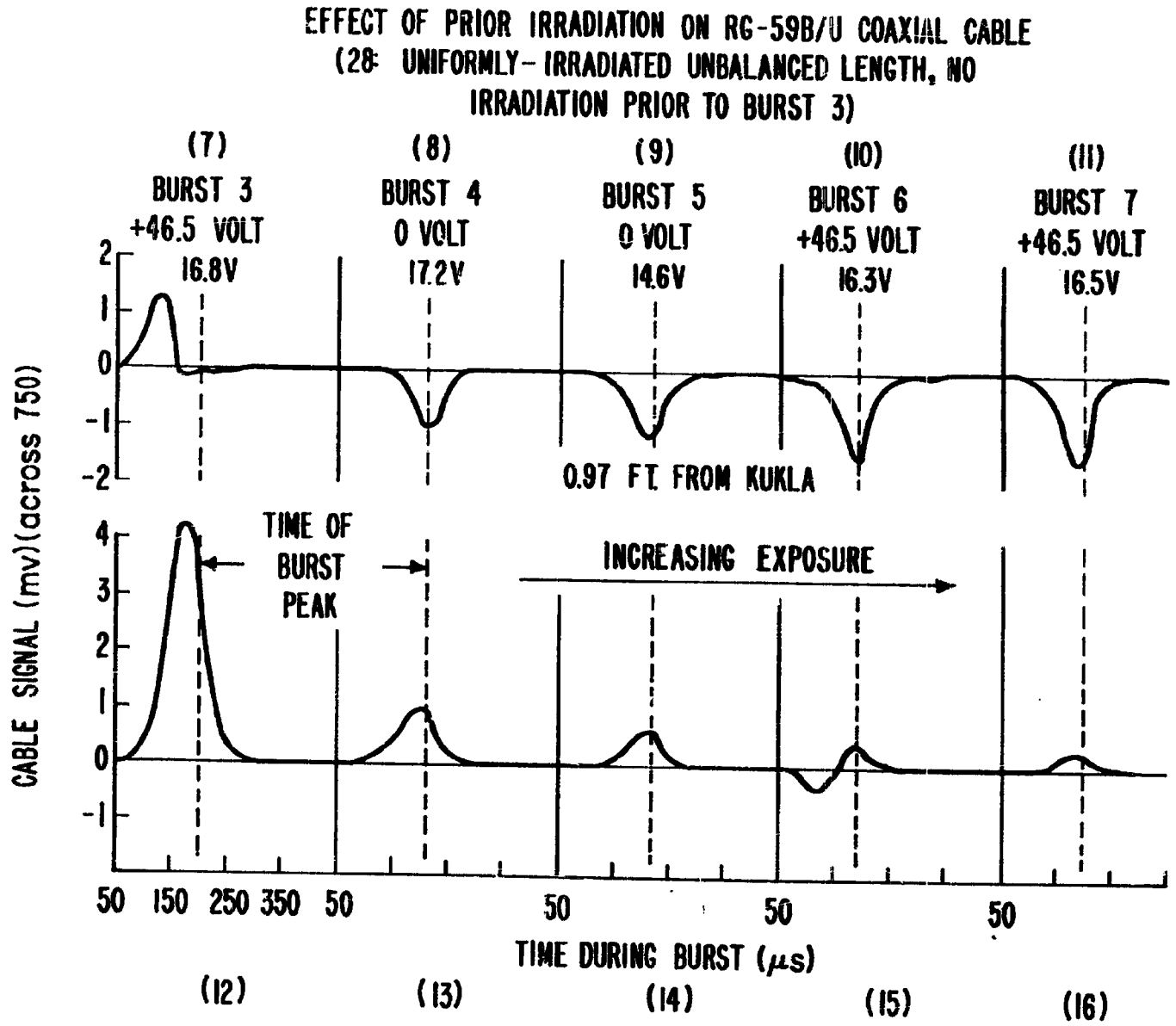
EFFECT OF PRIOR IRRADIATION ON RG-59B/U COAXIAL CABLE
(28 UNIFORMLY-IRRADIATED UNBALANCED LENGTH, NO
IRRADIATION PRIOR TO BURST 3)
(7)
BURST 3
+46.5 VOLT
16.8V
(8)
BURST 4
0 VOLT
17.2V
(9)
BURST 5
0 VOLT
14.6V
(10)
BURST 6
+46.5 VOLT
16.3V
(11)
BURST 7
+46.5 VOLT
16.5V
0.97 FT. FROM KUKLA
TIME OF
BURST
PEAK
INCREASING EXPOSURE
CABLE SIGNAL (mv)(across 750)
50 150 250 350 50 50 50 50
TIME DURING BURST (μs)
(12) (13) (14) (15) (16)

FIG. 13

VOLTAGE DEPENDENCE OF RADIATION-INDUCED CABLE SIGNALS IN 28' UNIFORMLY-IRRADIATED UNBALANCED LENGTH OF RG-59B/U COAXIAL CABLE

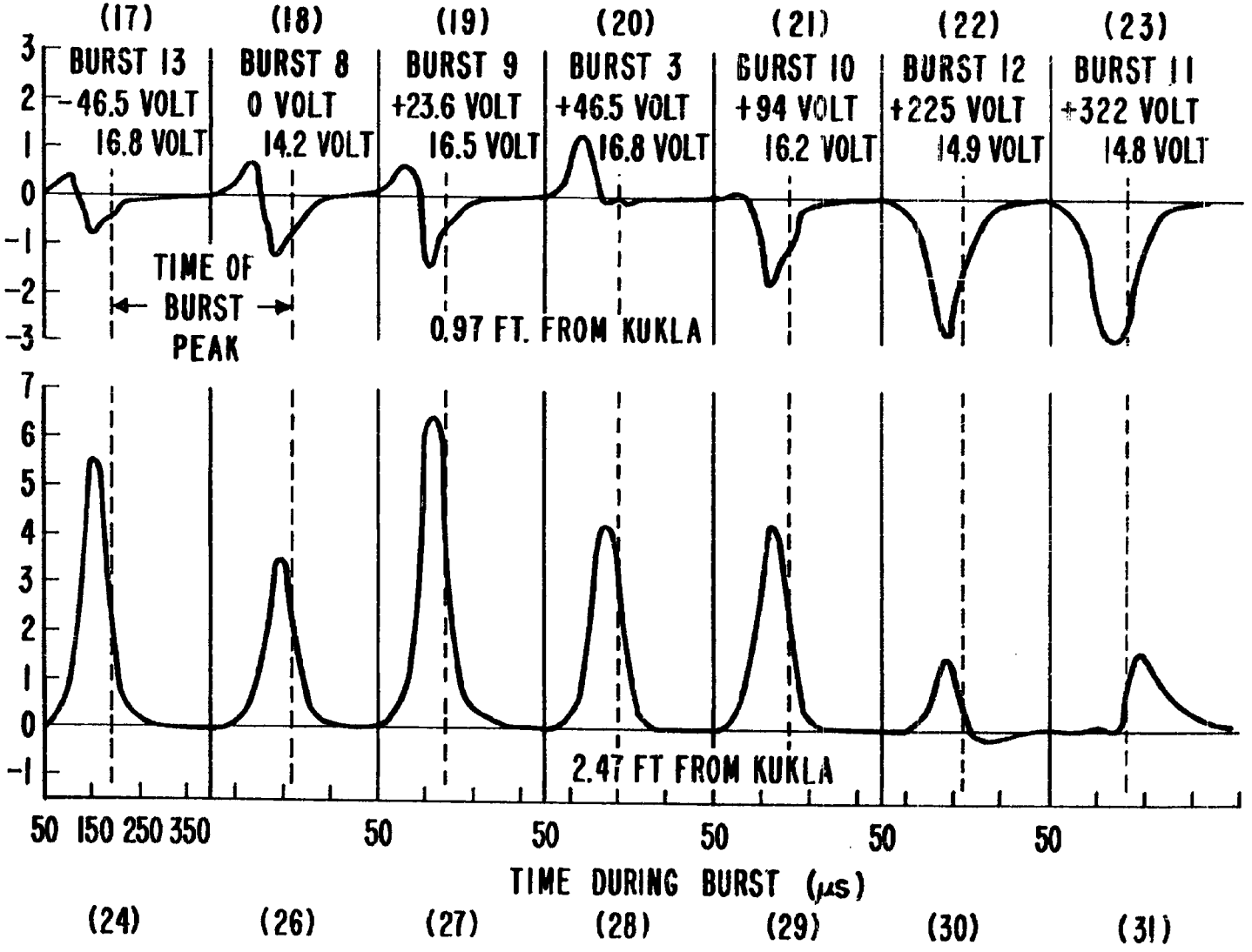

FIG. 14

ADDENDUM

After completion of this report a seminar on radiation effects was held at the U.S. Army Electronics Research and Development Laboratory, Fort Monmouth, New Jersey.

It was requested at this seminar, that the values of the dynamic cable parameters which were obtained from the response curves of Figure 12, with the dose rate values of Table II and Table III of Ref. 2, be correlated with the dosimetry data. This evaluation is carried out below using the procedures of Example 1 and the burst shape parameter $n = 2$, previously obtained with Example 2 of the text. Combining the characteristics of the response curves (2) and (6) of Figure 12 with the dosimetry data of Table II of Ref. 2, the following table can be arranged:

Table II - Ref. 2			Fig. 12		
Position Number	Avg. Specimen Distance from Kukla Center in Inches *	Gamma Intensity Relative to Position I Average Ratio	Response Number	Normalized Time of Peak Response X_1 Relative to Burst Peak- $X_o = 0.8$	Peak Current Response μA
1	12.3	1.00	1	---	---
2	29.8	0.24	2	$0.8\ \frac{9}{12} = 0.6$	$\frac{5.6mV}{75\Omega} = 75$
3	47.7	0.139	3	$0.8\ \frac{10}{12} = 0.66$	$\frac{4.2mV}{75\Omega} = 56$
4	65.6	0.083	4	$0.8\ \frac{11}{12} = 0.73$	$\frac{2.2mV}{75\Omega} = 29.4$
5	83.5	0.069	5	$0.8\ \frac{10}{12} = 0.66$	$\frac{1.5mV}{75\Omega} = 20$
6	101.5	0.066	6	$0.8\ \frac{11}{12} = 0.73$	$\frac{1.6mV}{75\Omega} = 21$

Formulas (13') (20) (20") and (20"') with T_2 = 70 microseconds in connection with formula (7'), are applicable to responses (2) to (6) of Fig. 12. From these formulas we obtain with (V) = 46.5 Volts

Position of Response Nr.	τ_m	$y(x_1)$	$[g(t)]_{max}$ Ω^{-1}	min MΩ	$[c_1(t)]_{max}$ μμF
2	0.097	$\frac{1}{[6.6]^2}$	1.6×10^{-6}	0.66	17
3	0.089	$\frac{0.97}{[6.6]^2}$	1.26×10^{-6}	0.8	13
4	0.058	$\frac{1}{[6.6]^2}$	0.63×10^{-6}	1.58	4.3
5	0.089	$\frac{0.97}{[6.6]^2}$	0.44×10^{-6}	2.26	4.6
6	0.058	$\frac{1}{[6.6]^2}$	0.46×10^{-6}	2.2	3.1

These results are now arranged with the corresponding Gamma peak rates using Table II Ref. 2 and Table III. With Burst 13 yielding a peak rate of 3.8×10^6 r/sec in position 1, the following correspondence table for Distance, Peak Gamma Rate, and Dynamic Resistance and Capacitance of the Cable Specimen is obtained.

Response or Position Nr.	Distances* (in inches)	Average Peak Gamma Rate in 10^6 r/sec	Minimum Dynamic Resistance in MΩ	Maximum Dynamic Capacitance Micro Microfarad
2	29.8	0.9	0.66	17
3	47.7	0.53	0.8	13
4	65.6	0.315	1.58	4.3
5	83.5	0.26	2.26	4.6
6	101.5	0.25	2.2	3.1

(* are approximately those shown on Fig.12)

The plots of minimum dynamic resistance (shown by data points marked x) and maximum dynamic capacitance(shown by data points marked (•) versus distance and average peak gamma rate are shown below:

The trends are seen very clearly. Linear dependence of dynamic conductance and capacitance from the gamma rate [case $|V| >> e_m$ for responses (2) to (6) of Fig 12] is valid.

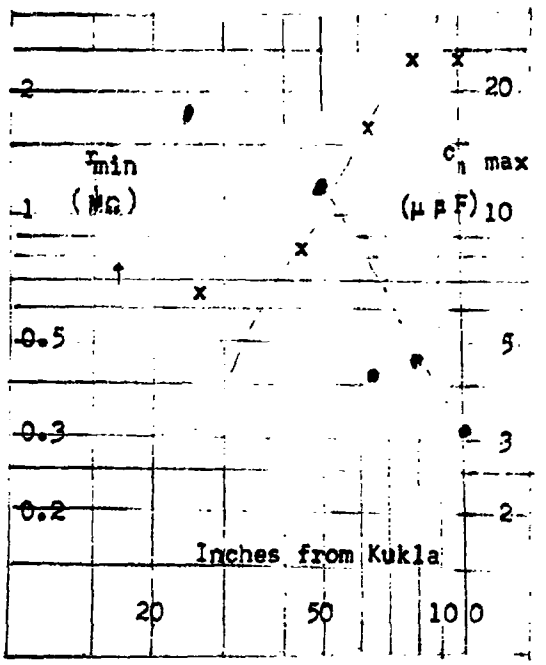

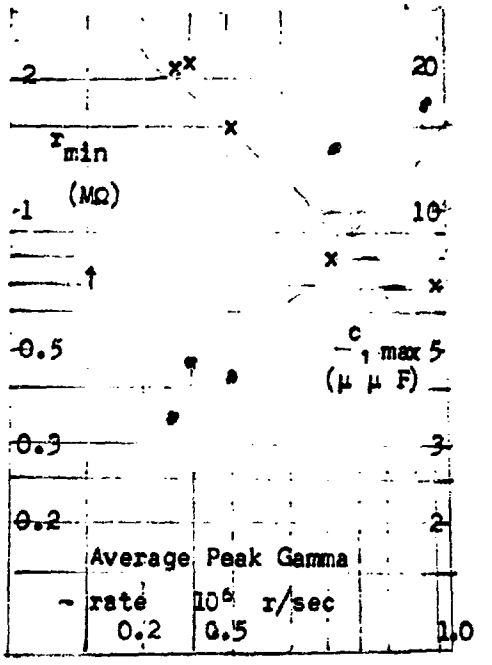

DISTRIBUTION

To	Copies
Commanding General U.S. Army Electronics Command ATTN: AMSEL-AD Fort Monmouth, New Jersey	1
Office of the Assistant Secretary of Defense (Research and Engineering) ATTN: Technical Library Room 3E1065, The Pentagon Washington 25, D.C.	1
Chief of Research and Development Department of the Army Washington 25, D.C.	2
Chief, United States Army Security Agency ATTN: ACofS, G4 (Technical Library) Arlington Hall Station Arlington 12, Virginia	1
Commanding General U.S. Army Electronics Research and Development Activity ATTN: Technical Library Fort Huachuca, Arizona	1
Commanding Officer U.S. Army Electronics Research and Development Activity ATTN: SELWS-AJ White Sands, New Mexico	1
Commanding Officer U.S. Army Electronics Materiel Support Agency ATTN: SELMS-ADJ Fort Monmouth, New Jersey	1
Headquarters, United States Air Force, ATTN: AFCIN Washington 25, D.C.	2
Commander Rome Air Development Center ATTN: RAALD Griffiss Air Force Base, New York	1
Ground Electronics Engineering Installation Agency ATTN: ROZMEL Griffiss Air Force Base, New York	1

To	Copies
Aeronautical Systems Division ATTN: ASAPRL Wright-Patterson Air Force Base, Ohio	1
U.S. Air Force Security Service ATTN: ESD San Antonio, Texas	1
Headquarters Strategic Air Command ATTN: DOCE Offutt Air Force Base Nebraska	1
Air Proving Ground Center ATTN: PGAPI Eglin Air Force Base, Florida	1
Air Force Cambridge Research Laboratories ATTN: CRXL-R Laurence G. Hanscom Field Bedford, Massachusetts	2
Air Force Systems Command, USAF ATTN: AFSC STLO NADC Johnsville, Pa.	1
Chief of Naval Research ATTN: Code 427 Department of the Navy Washington 25, D.C.	1
Bureau of Ships Technical Library ATTN: Code 312 Main Navy Building, Room 1528 Washington 25, D.C.	1
Chief, Bureau of Ships ATTN: Code 454 Department of the Navy Washington 25, D.C.	1

To	Copies
Chief, Bureau of Ships ATTN: Code 686B Department of the Navy Washington 25, D.C.	1
Director U.S. Naval Research Laboratory ATTN: Code 2027 Washington 25, D.C.	1
Commanding Officer & Director U.S. Navy Electronics Laboratory ATTN: Library San Diego 52, California	1
Commander U.S. Naval Ordnance Laboratory White Oak Silver Spring 19, Maryland	1
Director U.S. Army Engineer Research & Development Laboratories ATTN: Technical Documents Center Fort Belvoir, Virginia	1
Commanding Officer U.S. Army Chemical Warfare Laboratories ATTN: Technical Library, Building 330 Army Chemical Center, Maryland	1
Commander Armed Services Technical Information Agency ATTN: TIPCR Arlington Hall Station Arlington 12, Virginia	10
USAERADL Liaison Officer Ordnance Tank Automotive Command U.S. Army Ordnance Arsenal Detroit, Center Line, Michigan	1
USAERADL Liaison Officer Naval Research Laboratory ATTN: Code 1071 Washington 25, D.C.	1

To	Copies
USAERADL Liaison Office Massachusetts Institute of Technology Building 26, Room 131 77 Massachusetts Avenue Cambridge 39, Massachusetts	1
USAERADL Liaison Office Aeronautical Systems Division ATTN: ASDL-9 Wright-Patterson Air Force Base Ohio	1
U.S. Army Research Liaison Office Lincoln Laboratory P. O. Box 73 Lexington, Massachusetts	1
USAERADL Liaison Officer Rome Air Development Center ATTN: RAOL Griffiss Air Force Base	1
Chief, West Coast Office U.S. Army Electronics Research and Development Laboratory 75 South Grand Avenue, Building 13 Pasadena, California	1
USAEMSA Liaison Engineer Signal Section, Eighth U.S. Army A.P.O. 301 San Francisco, California	1
Chief Scientist, SELRA/SL-CS, Hq, USAERADL	1
Director of Research, SELRA/SL-DR	1
USAERADA-WHITE SANDS /Liaison Office, SELRA/SL-LNW, USAERADL	1
Corps of Engineers Liaison Officer, SELRA/SL-LNE, USAERADL	1
Marine Corps Liaison Officer, SELRA/SL-LNR, USAERADL	1
USA Combat Developments / Command Liaison Office, SELRA/SL-LNF, USAERADL	2

DISTRIBUTION (Cont)

To	Copies
Commanding Officer, U.S. Army Signal Research Activity Evans Area	1
Chief, Technical Information Division, Hq, USAERADL	6
Institute for Exploratory Research ATTN: Tech Staff	2
USAERADL Technical Documents Center, Evans Area	1
Mail and Record Unit Nr. 1	1
Exploratory Research Division C ATTN: Dr. Ikrath	20
Headquarters, Electronic Systems Division, ATTN: ESRR & ESSD, Laurence G. Hanscom Field, Bedford, Massachusetts	2
Boeing Airplane Company Seattle 24, Washington	1
Battelle Memorial Institute 505 King Avenue Columbus, Ohio	1
Edgerton, Germeshausen,& Grier 160 Brookline Avenue Boston 15, Mass.	1

Army, Ft. Monmouth, NJ-MON 4764-62

AD_____DIV_____

Army Electronics Research and Development Laboratory, Fort Monmouth, N. J.
Nuclear Pulse Effects in Cables, by K. Ikrath and R. Constantine, August 1962. 57 pp. incl. illus. 3 refs. (USAERADL Technical Report 2292)
(DA Task 3A99-25-003-02) Unclassified Report

An equivalent circuit for a piece of cable is developed and the differential equations of this circuit are solved under the conditions of a transient burst of nuclear radiation and under various ranges of cable bias voltage. Graphs of representative cases are represented and compared to experimental results. A method of solving for the transient change in cable parameters is given and sample calculations are shown.

UNCLASSIFIED

1. Nuclear Physics
2. Radiation Effects on Electrical Components
I. Ikrath, Kurt and Constantine, Randolph
II. Army Electronics Research & Development Laboratory, Fort Monmouth, N. J.
III. DA Task 3A99-25-003-02

UNCLASSIFIED

AD_____DIV_____

Army Electronics Research and Development Laboratory, Fort Monmouth, N. J.
Nuclear Pulse Effects in Cables, by K. Ikrath and R. Constantine, August 1962. 57 pp. incl. illus. 3 refs. (USAERADL Technical Report 2292)
(DA Task 3A99-25-003-02) Unclassified Report

An equivalent circuit for a piece of cable is developed and the differential equations of this circuit are solved under the conditions of a transient burst of nuclear radiation and under various ranges of cable bias voltage. Graphs of representative cases are represented and compared to experimental results. A method of solving for the transient change in cable parameters is given and sample calculations are shown.

UNCLASSIFIED

1. Nuclear Physics
2. Radiation Effects on Electrical Components
I. Ikrath, Kurt and Constantine, Randolph
II. Army Electronics Research & Development Laboratory, Fort Monmouth, N. J.
III. DA Task 3A99-25-003-02

UNCLASSIFIED

AD_____DIV_____

Army Electronics Research and Development Laboratory, Fort Monmouth, N. J.
Nuclear Pulse Effects in Cables, by K. Ikrath and R. Constantine, August 1962. 57 pp. incl. illus. 3 refs. (USAERADL Technical Report 2292)
(DA Task 3A99-25-003-02) Unclassified Report

An equivalent circuit for a piece of cable is developed and the differential equations of this circuit are solved under the conditions of a transient burst of nuclear radiation and under various ranges of cable bias voltage. Graphs of representative cases are represented and compared to experimental results. A method of solving for the transient change in cable parameters is given and sample calculations are shown.

UNCLASSIFIED

1. Nuclear Physics
2. Radiation Effects on Electrical Components
I. Ikrath, Kurt and Constantine, Randolph
II. Army Electronics Research & Development Laboratory, Fort Monmouth, N. J.
III. DA Task 3A99-25-003-02

UNCLASSIFIED

AD_____DIV_____

Army Electronics Research and Development Laboratory, Fort Monmouth, N. J.
Nuclear Pulse Effects in Cables, by K. Ikrath and R. Constantine, August 1962. 57 pp. incl. illus. 3 refs. (USAERADL Technical Report 2292)
(DA Task 3A99-25-003-02) Unclassified Report

An equivalent circuit for a piece of cable is developed and the differential equations of this circuit are solved under the conditions of a transient burst of nuclear radiation and under various ranges of cable bias voltage. Graphs of representative cases are represented and compared to experimental results. A method of solving for the transient change in cable parameters is given and sample calculations are shown.

UNCLASSIFIED

1. Nuclear Physics
2. Radiation Effects on Electrical Components
I. Ikrath, Kurt and Constantine, Randolph
II. Army Electronics Research & Development Laboratory, Fort Monmouth, N. J.
III. DA Task 3A99-25-003-02

UNCLASSIFIED